Atomic Spectroscopy

May/June 2001 Volume 22, No. 3

In This Issue:

ASPND7 22(3) 299–330 (2001)
ISSN 0195-5373

Issues also available electronically.

(see inside front cover)

Atomic Spectroscopy
Vol. 22(3), May/June 2001

Printed in the United States and published six times a year by:

PerkinElmer Instruments
710 Bridgeport Avenue
Shelton, CT 06484-4794 USA
www.perkinelmer.com

SUBSCRIPTION INFORMATION

Atomic Spectroscopy
P.O. Box 3674
Barrington, IL 60011 USA
Fax: +1 (847) 304-6865

2000 Subscription Rates

- U.S. $60.00 includes third-class mail delivery worldwide; $20.00 extra for electronic file.
- U.S. $80.00 includes airmail delivery; $20 extra for electronic file.
- U.S. $60.00 for electronic file only.
- Payment by check (drawn on U.S. bank in U.S. funds) made out to: "*Atomic Spectroscopy*"

On-line Access

- For electronic file, send request via e-mail to: atsponline@yahoo.com

Back Issues/Claims

- Single back issues are available at $15.00 each.
- Subscriber claims for missing back issues will be honored at no charge within 90 days of issue mailing date.

Address Changes to:

Atomic Spectroscopy
P.O. Box 3674
Barrington, IL 60011 USA

Microfilm

Atomic Spectroscopy issues are available from:
University Microfilms International
300 N. Zeeb Road
Ann Arbor, MI 48106 USA
Tel: (800) 521-0600 (within the U.S.)
+1 (313) 761-4700 (internationally)

Guidelines for Authors

Atomic Spectroscopy serves as a medium for the dissemination of general information together with new applications and analytical data in atomic absorption spectrometry.

The pages of *Atomic Spectroscopy* are open to all workers in the field of atomic spectroscopy. There is no charge for publication of a manuscript.

The journal has around 3000 subscribers on a worldwide basis, and its success can be attributed to the excellent contributions of its authors as well as the technical guidance of its reviewers and the Technical Editors.

A manuscript can be submitted to the editor by mail or e-mail in the following manner:

1. Triplicate, double-spaced.
2. Include abstract for articles.
3. Number the references in the order they are cited in the text.
4. Include bibliography.
5. Submit original drawings or glossy photographs and figure captions.
6. Consult a current copy of *Atomic Spectroscopy* for format.
7. E-mail text in .doc file and graphics in .tif files to the editor: anneliese.lust@perkinelmer.com

All manuscripts are sent to two reviewers. If there is disagreement, a third reviewer is consulted.

Minor changes in style are made in-house and submitted to the author for approval.

A copyright transfer form is sent to the author for signature.

If a revision of the manuscript is required before publication can be considered, the paper is returned to the author(s) with the reviewers' comments.

In the interest of speed of publication, a typeset copy is faxed to the corresponding author for final approval.

After publication, the senior author will receive 50 complimentary reprints of the article.

Additional reprints can be purchased, but the request must be made at the time the manuscript is approved for publication.

Anneliese Lust
Editor, *Atomic Spectroscopy*
PerkinElmer Instruments
710 Bridgeport Avenue
Shelton, CT 06484-4794 USA

A Routine Quality Control Method for the Determination of Iodine in Human and Pet Food by ICP-MS

D. Andrey
Department of Quality and Safety Assurance, Nestlé Research Center, P.O. Box 44
Vers chez-les–Blanc, CH-1000 Lausanne 26, Switzerland
P. Zbinden*, M. Kwok Wah, and W. Lee
Nestlé R&D Center, Singapore RQAL, 29, Quality Road, 618802 Singapore

ABSTRACT

A rapid, robust ICP-MS method is described for the determination of iodine in human as well as pet food. The sample preparation is made by alkaline hydrolysis with tetramethylammonium hydroxide using either microwave heating or the high pressure asher. Method validation was carried out using seven reference food materials with certified iodine content, and by cross-validation with gas chromatography, neutron activation analysis, and colorimetry. The method has been proven to give accurate and repeatable results for a range of fortified human and pet food products, and to be useful in the environment of a central quality control laboratory.

INTRODUCTION

Iodine is one of the most important elements in human nutrition. Its concentration in foods needs to be controlled because the recommended daily intake, ranging from 150-200 µg/day, is not always achieved. Iodine deficiency may cause mental retardation, brain damage, goitre, or poor physical development. Iodine deficiency disorder continues to affect a large number of people in the world. In 1993, the World Health Organization (WHO) (1) estimated that iodine deficiency is a significant public health problem in 118 countries.

The main source of iodine in nutrition is fish and seafood. Milk is another important source of iodine. Supplementing food with iodide or iodate has already been used for many years in developed countries and more recently in developing countries. Table salt is often fortified with iodide or iodate. Milk-based infant formula and other dietetic products, where iodine levels are fortified, are also good sources of iodine. Iodine may also be fortified in certain culinary products such as seasoning or stocks. Pet foods are also fortified, particularly cat food, since cats are very sensitive to iodine deficiency.

An excess of iodine in the diet may lead to hyperthyroidism and other adverse effects, which can be almost entirely avoided by adequate and sustained quality control and monitoring of iodine supplements. A good quality control of fortified foods is important to ensure that the iodine is present within the norms given by local legislation. With respect to analysis, these fortified food products are a challenge to the analytical chemist. Therefore, the methodology must be robust enough to be applicable to a large range of food products.

Analytical techniques often used for routine analysis in the food industry include colorimetry (2,3), gas chromatography (GC) (4), ion selective electrode (ISE) (5), and high-performance liquid chromatography (HPLC) (6). These methods have certain limitations because they are time-consuming, suffer from matrix effects, and are not applicable to all product types. Neutron activation analysis (7), which is considered as a reference method, cannot be used in a routine environment because of its complexity and the need for a nuclear reactor.

In recent years, inductively coupled plasma mass spectrometry (ICP-MS) has emerged as a useful method for the quantification of iodine (8-19), since it has excellent sensitivity and selectivity towards iodine. Considerable effort has gone into comparing and optimizing the various sample preparation methods available for this analysis (11,12). When using normal acid mineralization with nitric acid, some losses of iodine may occur since hydrogen iodide (HI) is gaseous at room temperature and therefore volatile (Figure 1). The volatility of iodine (I2) may also lead to severe memory problems in

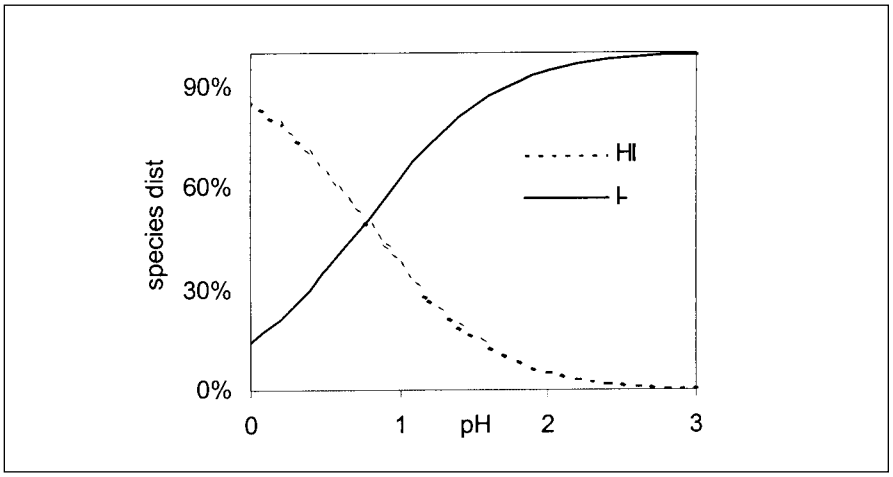

Fig. 1. Iodine distribution according to the pH. $K_a = 1.69 \cdot 10^{-1}$

*Corresponding author.

the sample introduction system of the ICP-MS (10). To overcome these problems, a number of approaches have been used. Mineralization using nitric acid should include some perchloric acid to convert the volatile iodide into non-volatile iodate (10), but even so, the iodine analysis must be completed on the same day because of the reconversion to volatile iodine. Other approaches include oxygen ashing (11,12,16) or the use of alkaline digestion with tetramethylammonium hydroxide (TMAH) (14,15,18). A recent ring test was performed for the determination of iodine by ICP-MS with TMAH digestion (13,14) and the procedure has been approved as an official method in Germany (18).

The objective of the present work was to develop a rapid ICP-MS method, applicable to a wider range of fortified food products including culinary, dietetic, and clinical nutrition products and pet foods. The alkaline extraction method using TMAH was evaluated and applied to a large range of commercial foods, including high-salt products.

EXPERIMENTAL

Sample Preparation

The microwave systems used were an MDS 2000 microwave system (CEM Corporation) with 12-position support and maximum power at 800 W or an MLS 1200 Mega microwave system (Milestone) with 10-position support and maximum power at 1200 W.

These microwave systems were used with either 50-mL volumetric glass flasks or 100-mL glass beakers.

Another decomposition scheme used was an HPA-S High Pressure Asher™ (PerkinElmer Instruments) using maximum pressure of 150 bar, maximum temperature at 320ºC, and 15-mL quartz vessels.

Instrumentation

The ICP-MS instruments used were a PerkinElmer SCIEX ELAN® 6000 and ELAN 6100 (PerkinElmer SCIEX, Concord, Ontario, Canada). A thermostated Cinabar (mini-cyclonic) spray chamber (16°C) with a Micromist nebulizer (sample flow = 0.2 mL/min, from Glass Expansion, Australia) was used for sample introduction. Other ICP-MS analytical parameters for the ELAN 6000 can be found in Table I. Similar conditions were used for the ELAN 6100.

Data acquisition was made using ELAN software v. 2.2 based on the Microsoft® Windows NT® operating system.

Other equipment used included:

-- Mixing manifold for the addition of an internal standard (PerkinElmer, part number B050-7957).

-- Disposable syringe filters, 0.2 µm (MINISART, Sartorius), non-sterile.

-- Polypropylene tubes, 50 mL (Falcon #352070).

-- Polystyrene tubes 14 mL (Falcon #322059).

-- Volumetric flask, glass, 50 mL, class A.

-- Volumetric flask, glass, 200 mL, class A.

-- Beakers, tall-form, 100 mL.

-- Teflon® strip.

-- Glass cover (watch glass).

Reagents and Standards

Ultrapure water (18.2 MΩ, MilliQ™ Plus system).

Tetramethylammonium hydroxide solution (25%) in water (Purum, Fluka).

A 1 % TMAH (v/v) solution was prepared by diluting 4 mL TMAH (25%) to 100 mL with ultrapure water.

A stock solution (1000 mg/L) of iodine in 1% (v/v) TMAH solution was prepared from potassium iodide Suprapur (Merck). Dilutions were made each working day with 1% (v/v) TMAH to provide calibration solutions in the range 0-20 µg iodine/L.

Stock solutions (1000 mg/L) of germanium and tellurium were obtained from Merck, while rhodium and indium were obtained from High Purity Standards. They were diluted with 1% (v/v) TMAH solution to obtain the required concentrations.

Comparative Methods

The following methods used in the present work for cross-validation of the ICP-MS method have been described in the literature: colorimetric method (3), gas chromatography (GC) (4), and neutron activation analysis (NAA) (7).

TABLE I
Parameters for ELAN 6000 ICP-MS

Power	1300 W
Sweeps/reading	40
Reading / Replicates	1
Replicates	3
Analytical mass, Iodine	126.9000
Internal standard (Germanium) mass	73.9219
Scan mode	Peak hopping
Nebulizer, Argon flow	0.9 mL/min

Products Analyzed

Various commercial fortified food products were used for method development and validation: milk powders, stocks, spices, salt, dietetic infant formulas, mineral and vitamin premixes, clinical nutrition products, meal replacement products, and wet and dry pet food.

Reference Materials

- -- Whole Egg Powder, NIST 8415
- -- Bovine Muscle Powder, NIST 8414
- -- Corn Bran, NIST 8433
- -- Whole Milk Powder, NIST 8435
- -- Non-Fat Milk Powder, NIST 1549
- -- Milk Powder, BCR 150
- -- Spiked Skim Milk Powder, BCR 151

Sample Preparation: Microwave/Alkaline Hydrolysis With TMAH

Human Food Samples

Test portions (400 mg) of solid products or 1 g liquid product were accurately weighed into 50-mL volumetric flasks. Then, 10 mL of ultrapure water and 2 mL of TMAH were added. The flasks were closed with a Teflon strip and heated according to the program described in Table II. After 30 minutes in the microwave system, the flasks were allowed to cool to room temperature and made up to volume (50 mL) with ultrapure water. After shaking the solutions well, they were filtered through 0.2-µm disposable syringe filters into polystyrene tubes (14 mL) before ICP-MS analysis.

Pet Foods

A modified procedure was used for pet foods. The test portion was increased to 10 g (to overcome problems of non-homogeneity) and weighed into a 100-mL tall-form beaker, which was then covered with a watch glass. Test portions were heated twice for 30 minutes in the microwave system (program given in Table II). The resulting suspension was transferred into a 200-mL volumetric flask and made up to volume with ultrapure water. After thorough shaking, a 10-mL aliquot was filtered through a 0.2-µm disposable syringe filter into a polystyrene tube (14 mL). The sample solutions were further diluted with 1% (v/v) TMAH solution before ICP-MS analysis to obtain an iodine content within the calibration range.

Salt (NaCl)

Test portions of 1 g were accurately weighed into 100-mL volumetric flasks and dissolved in 4 mL of TMAH (25%). The volume was adjusted to the 100-mL mark with ultrapure water. The sample solutions were further diluted with 1% (v/v) TMAH solution to obtain an iodine content within the calibration range.

Alkaline Digestion Using HPA-S (not applicable for pet foods)

A test portion of 300 mg of a solid sample or 1 g of liquid sample was weighed into a 15-mL HPA-S vessel. One mL or 2 mL of TMAH solution (25%) was added. The test portion was mixed with a vortex mixer. The vessels were sealed using a Teflon strip and quartz lids. Up to twenty-one 15-mL vessels were placed in the HPA-S autoclave and heated under pressure using the program listed in Table III.

The samples were diluted to 10 mL with ultrapure water. After shaking them well, they were filtered through 0.2-µm disposable syringe filters into polystyrene tubes (14 mL) before ICP-MS analysis. The sample solutions were further diluted with 1% TMAH solution to obtain an iodine content within the calibration range.

TABLE II
Microwave Heating Programs for Alkaline Hydrolysis With TMAH

Number of flasks	MW program for CEM 2000 (max power 800W) (% Power)	MW program for Milestone MLS 1200 (W)
2	5	40
3	9	60
4	13	80
5	17	100
6	21	120
7	25	140
8	29	160
9	33	180
10	37	200
11	41	Not applicable
12	45	Not applicable

TABLE III
HPA-S Heating Program

Start temperature (ºC)	Ramp time (min)	Temperature 2 (ºC)	Hold time (min)
RT	20	90	10
90	10	120	30
120	Fast	RT	End

Total time 50 min

RESULTS AND DISCUSSION

Validation of the analytical method for iodine by ICP-MS was rather difficult for certain types of matrices because of the lack of food reference materials with certified iodine content. Moreover, the standard addition method, if very useful, was not sufficient to fully validate the method. To complete the validation, it was decided to compare the ICP-MS results with those from other established analytical methods already available for iodine. Three other methodologies were used for comparison: GC (4), NAA (7), and a catalytic colorimetric method (3). Due to some limitations of these methods, the results were not available for all the matrices studied here.

Analytical Performance of the Method

Limits of Detection and Quantification

These limits were evaluated on standard solutions and are shown in Table IV. They were calculated using the following equation:

$$L_{OD/OQ} = \frac{[Std]}{I_{Std} - I_{back}} * StDev_{Back} * Fstat$$

Where :

$L_{OD/OQ}$ = Detection (D) and quantification limit (Q)

Fstat = Statistical factor: 3 for the detection limit and 10 for the quantification limit

[Std] = Concentration of the iodine standard (2 µg/L)

I_{std} = Raw intensity of standard solution

I_{Back} = Background raw intensity measured on a blank

$StDev_{Back}$ = Standard deviation measured on I_{Back}

TABLE IV
Detection Limits (LOD) and Quantification Limits (LOQ)

LOD	in solution	0.04 µg/L
LOQ	in solution	0.12 µg/L
LOQ	in pet food	25 µg/kg
LOQ	in human food	15 µg/kg

Repeatability and Intermediate Reproducibility

Global repeatability (r) and intermediate reproducibility (R) at the 95% confidence level were evaluated on milk powders and stock cubes. The median (r), based on the analysis of 38 food products between 26 and 4500 µg/kg, was 1% relative, while the average (r) was 9% relative. Pet foods were evaluated separately because of the heterogeneity of the products. The median (r) was 4% relative, while the average (r) was 5% relative based on the analysis of six pet food products between 60 and 2180 µg/kg of iodine.

The intermediate reproducibility was evaluated by measuring a series of samples on five different days in the same laboratory. For human foods, four products were analyzed with a median (R) of 3% relative and an average (R) of 10% relative. In the case of pet foods, six different samples were analyzed with a median (R) of 7% relative and an average (R) of 9% relative.

Analysis of Certified Reference Material

As shown in Table V, the results obtained by ICP-MS for a series of

TABLE V
Determination of Iodine in Certified Reference Materials and In-house Reference Materials (Comparison of results (µg/kg) obtained by different analytical techniques.)

Sample name	Ref. value	ICP-MS Microwave	n	ICP-MS HPA-S	n	GC	n	Colorimetry	n
Whole egg powder *NIST 8415*	1970±460	1968±6	3	*n.a.*		*n.a.*		1877±23	2
Bovine Muscle powder *NIST 8414*	35±12	29±1	3	*n.a.*		*n.a.*		*n.a.*	
Corn Bran *NIST 8433*	26± 6	28±6	5	*n.a.*		*n.a.*		*n.a.*	
Whole milk powder *NIST 8435*	2300±400	2526±47	3	*n.a.*		*n.a.*		2233±257	2
Non Fat Milk powder *NIST 1549*	3380±200	3511±32	3	*n.a.*		*n.a.*		3301± 34	2
Milk powder *BCR 150*	1290± 90	1333±4	3	*n.a.*		*n.a.*		*n.a.*	
Spiked Skimmed Milk powder *BCR 151*	5350±140	5355±115	3	5324±46	6	*n.a.*		4571±115	2
Milk powder, Nestlé *DDP 199*	930±84	932±9	3	*n.a.*		890	1	676 ± 88	2
Milk powder, Nestlé *DDP 299*	1120±101	1086±10	3	*n.a.*		980	1	933±107	2
Milk powder, Nestlé *DDP 399*	980±150	836±22	3	*n.a.*		790	1	651±67	2
Milk powder, Nestlé *DDP 499*	960±140	1025±67	3	872±41	8	870	1	699	1

n.a. = not analyzed.
n = Number of replicate analyses.

seven certified food materials are in very good accordance with the reference values. In this table, comparative results obtained in the same laboratory, using GC or colorimetry, can also be found.

Analysis of Fortified Culinary Products and Salt (NaCl)

Culinary products such as stock cubes and seasonings are more difficult matrices because they contain high concentrations of salt and fat. Inorganic salts are known to produce strong matrix effects on ICP-MS analysis.

The choice of the internal standard for this type of sample was crucial. Various authors (13,14,16) have reported the use of tellurium (Te^{128}) as an internal standard, since it has a similar mass to that of iodine. This internal standard was found to be very suitable for most digested food samples but was less efficient for high-salt products and resulted in an overestimation of the iodine concentration. After investigating several internal standards (Ge, In, Rh, and Te), germanium (Ge^{74}) was found to be the best compromise for all types of samples, including products with a high-salt content. Figure 2 shows that Ge^{74} used as an internal standard gives a better correction for iodine analyses in solutions of high-salt concentrations than Te^{128}.

Since no reference samples were available for culinary products, a comparison of results obtained by colorimetry, GC, and ICP-MS was made. As shown in Table VI, similar results were obtained by all three methods for most product types. However, both the GC and the colorimetric methods were hindered by interferences when products with spices were analyzed, thus resulting in an under-estimation of iodine content and poor repeatability of the results. One reason for this could be the differences in the preparation step between the three methods. The GC and colorimetric

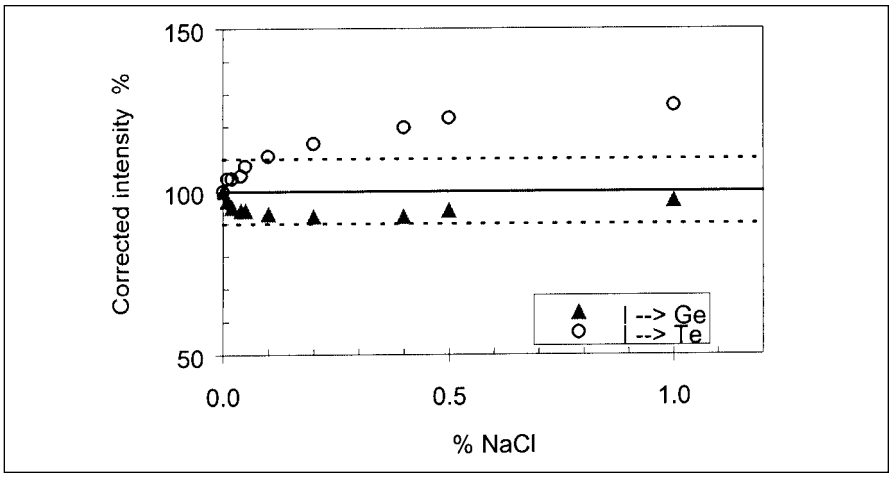

Fig. 2. Intensities of iodine in salt solution corrected by germanium or tellurium. Iodine concentration 10 µg/L; germanium and tellurium concentrations 50 µg/L.

TABLE VI
Comparison of Several Methods for Iodine Content (µg/kg) in Culinary Products

Sample	Origin[a]	State	ICP-MS[b] (HPA-S)	n[c]	GC	n	Colorimetry	n
Vegetable stock	CH	Moist	3970±226	2	n.a.[d]		3941±40	3
Beef stock	CH	Moist	4103±36	2	n.a.[d]		4366±45	3
			4377±116	**6**				
Beef stock	CH	Moist	5173±172	2	n.a.[d]		5353±12	3
Chicken stock	CH	Moist	4447± 90	2	n.a.[d]		3375±70	3
Stock cube	CH	Moist	4715±195	6	n.a.[d]		4400±140	3
			4566±171	**6**				
Stock cube	Af	Moist	33681±422	2	n.a.[d]		31300±1550	21
Stock cube	CH	Moist	4715±196	6	n.a.[d]		4871±306	2
Stock cube	Ph	Moist	22383±2135	4	20501±3895	11	20972±2580	2
			25926±612	**6**				
Stock cube	Ph	Moist	22362±2532	4	18064±104	2	19695±2047	2
Stock cube	Ph	Moist	20983±1991	4	17160±544	2	17636±800	2
			23802±158	**2**				
Stock cube	Ph	Moist	20488±2652	4	18018±277	2	19234±411	2
Spice	Ph	Dry	22595±1032	8	5073±2537[e]	12	15838±1966	2
Liquid seasoning	Ph	Liquid	10616±688	4	12280±571	4	10139±1589	2
			11679±387	**2**				
Liquid garlic	Ph	Liquid	9613±765	4	11425±393	4	9053±488	2
			10572±30	**2**				

[a]Country of origin of product: CH = Switzerland, Ph = Philippines, Af = Africa.
[b]Under column "ICP-MS" **Underlined & bold** results, sample preparation with HPA-S. All other results from ICP-MS were obtained using microwave alkaline hydrolysis.
[c]n = Number of replicate analyses.
[d]n.a. = not analyzed.
[e]= interferences.

methods only determine free and not bound iodine. In contrast, dissolution with TMAH, allied to microwave heating prior to ICP-MS measurement, seems to give a more complete recovery because of the partial destruction of the matrix. A comparison was made between ICP-MS and colorimetric values for culinary products with an R^2 = 0.9920. One product containing spices was omitted from the calculation.

Pet Food Products

Commercial pet foods can be considered similar to culinary products, since they may contain high concentrations of salt. No certified reference pet food samples were available. The validation of the ICP-MS method for this type of product was made either by comparison of the results from neutron activation analysis, colorimetry, or by standard addition (added as KI). Standard addition was performed on three dry and 10 wet pet food products. The measured recoveries were 90 ± 6% (min=79%, max=103%) as shown in Table VII. A correlation of R^2=0.9777 was found between the results obtained by ICP-MS and NAA (Table VIII, Figure 3) on a series of dry cat foods.

Premixes

Fortification of iodine in food products normally occurs via the addition of a concentrated premix containing iodine as well as various other minerals and/or vitamins. A carrier is used such as maltodextrin or salt to aid in the homogeneous distribution of iodine in the food product. The main problem in the analysis of these premixes is their relative heterogeneity. A comparison is made in Table IX between values obtained by a GC method and ICP-MS. The results between the two methods are similar and within the expected range.

TABLE VII
Recovery of Iodine From Spiked Pet Foods
(All samples were spiked to give 5 µg/L of iodide in analytical solution.)

Product description and ingredients	State	Cat or Dog	Iodine in product (µg/kg)	Spike recovery (%)
Meat, beef	Dry	Cat	1965	101,103
Chicken, duck, rabbit	Dry	Cat	1445	85 ,87
Turkey, beef, chicken	Dry	Cat	1315	86, 95
Beef, lamb	Wet	Cat	553	84,91,94,79
Duck, turkey	Wet	Cat	305	88, 82
Salmon	Wet	Cat	10410	87, 95
Beef, chicken	Wet	Cat	608	88,79, 87, 98
Game, tomato, courgette	Wet	Cat	717	96, 92
Salmon, hake	Wet	Cat	801	87, 93
Beef, poultry	Wet	Cat	529	86, 91
Salmon, tuna	Wet	Cat	803	93, 93
Lamb, poultry	Wet	Dog	880	88, 93
Beef, liver	Wet	Dog	955	85, 82
			Median	88%
			Average	90%
			No. analyses	30
			RSD	6%

TABLE VIII
Comparison of Results for the Determination of Iodine in Dry Cat Food by ICP-MS and Neutron Activation Analysis (Results by colorimetry are also given.)

Sample #	Neutron Activation (µg/kg)	ICP-MS (µg/kg)	Colorimetry (µg/kg)
1	2120±230	2287±205	1894 ± 21
2	2180±230	2108±71	2020±2
3	1270±130	1205±28	1298±136
4	1820±180	1622±88	2030±146
5	60±11	53±5	62±13

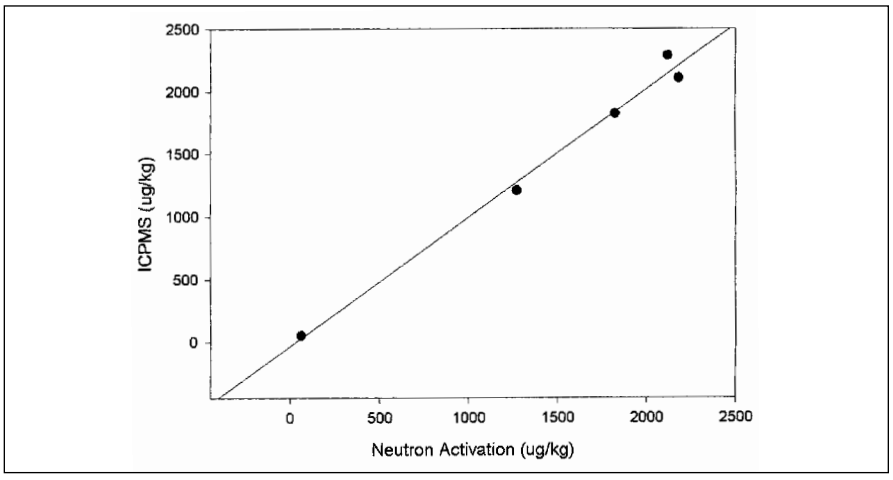

Fig. 3. Correlation between neutron activation analysis and ICP-MS for the determination of iodine in dry pet food.

Atomic Spectroscopy
Vol. 22(3), May/June 2001

Fortified Nutritional Products

A comparison was made between the results by GC and ICP-MS for a series of clinical nutrition and meal replacement products (Table X). Similar results were obtained.

CONCLUSION

A robust analytical method for the determination of total iodine in food products, including pet food, has been developed and validated. This method is based on an alkaline (TMAH) digestion using heating in a microwave oven or with HPA-S. The quantification of iodine was carried out by ICP-MS at mass I^{127}, using Ge^{74} as the internal standard. Validation of the method was carried out on seven certified reference materials. Good agreement with reference values was obtained. The method was also cross-validated by comparison of the results on a large range of fortified food products and pet foods with those obtained by NAA, GC, and a colorimetric method. Compared to the other methodologies, the ICP-MS procedure shows clear advantages, because it is applicable to a large range of food products as well as being more rapid and easier to use.

ACKNOWLEDGMENTS

The authors would like to thank Dr A.R. Byrne and co-workers of the Joseph Stefan Institute of the Ljubljana University in Slovenia for performing the analyses of iodine by neutron activation analysis.

Received April 13, 2001.

REFERENCES

1. WHO/UNICEFF/ICCIDD (1993) Global prevalence of iodine deficiency disorders. Micronutrient deficiency information systems (MDIS). Working paper No.1, WHO, Geneva, Switzerland.
2. .E. Moxon and E.J. Dixon, Analyst 105, 344 (1980).
3. L.Perring, M.Basic-Dvorzak, and D. Andrey, Analyst (in publication).
4. T. Stijve, J-M.Diserens, and C.J. Blake, Deutsche Lebens. Rundsch. 84 (11), 341 (1988).
5. J.T. Tanner, S.A. Barnett, and K.Mountford, J. AOAC Int. 76 (5), 1024 (1993).
6. D.Sertl and W.Malone, J. AOAC Int. 76 (4), 711 (1993).
7. M. Dermelj, Z. Slejkovec, A.R.Byrne, P.Stegnar, V.Stibilj, and R. Rossbach, Fresenius' J. Anal. Chem. 338, 559 (1990).
8. W. Lee, K.S. Park, S.T.Kim, and Y.M. Kim, Anal. Sci.Technol. 12(6), 528 (1999).
9. J. Yoshinaga, Bunseki (4), 332 (1999).
10. E.H. Larsen, P. Knuthsen, and M. Hansen, J. Anal. At. Spectrom. 14(1), 41 (1999).
11. Y. Gelinas, G.V. Iyengar, and R.M. Barnes, Fresenius' J. Anal. Chem. 362 (5), 483 (1998).
12. G. Knapp, B. Maichin, P.Fecher, S.Hasse, and P. Schramel, Fresenius' J. Anal. Chem. 362 (6), 508 (1998).
13. P.A. Fecher, I. Goldmann, and A. Nagengast, J. Anal. At. Spectrom. 13(9), 977 (1998).
14. P. Fecher, C. Walther, and J. Sondermann, Deutsche Lebensm. Rundschau 95 (4), 133 (1999).
15. G. Radlinger and K.G. Heumann, Anal. Chem. 70 (11), 2221 (1998).
16. Y. Gelinas, A. Krushevska, and R.M. Barnes, Anal. Chem. 70 (5), 1021 (1998).
17. K. M. Eckhoff and A. Maage, J. Food Composit. Anal. 10 (3), 270 (1997).
18. LMBG, Analysis of foods. Determination of iodine in dietetic foods by ICP-MS (MS with inductively coupled plasma). Amtliche-Sammlung-von-Untersuchungsverfahren-nach-Paragraph-35-LMBG; L 49.00-6 (1998).
19. E.H. Larsen and M.B. Ludwigsen, J. Anal. At. Spectrom. 12 (4), 435 (1997).

TABLE IX
Comparison of ICP-MS and GC for Iodine Content (mg/kg) in Premixes Used for Product Supplements

Premix type	GC (mg/kg)	n	ICP-MS (mg/kg)	n
Vitamin premix 1	172	1	193±7	2
Vitamin premix 2	223	1	279±27	2
Vitamin premix 3	82	1	93±2	2
Vitamin premix 4	95	1	91±3	2
Vitamin premix 5	179	1	186±3	2
Vitamin premix 6	145	1	174±5	2
Cat-food premix 1	49	1	41±2	2
Cat-food premix 2	43	1	47±1	2

n = Number of replicate analyses.

TABLE X
Comparison of ICP-MS and GC Methods for Iodine Content (mg/kg) in Fortified Nutritional Products

Product	GC (mg/kg)	n	ICP-MS (mg/kg)	n
Chicken soup mix	0.84	1	0.74±0.26	7
Fortified berry juice	0.15	1	0.12±0.004	4
Fortified orange juice	0.15	1	0.12±0.008	4
Infant formula (concentrate)	0.71	1	0.60±0.08	7
Infant formula (ready to feed)	0.14	1	0.13±0.012	2
Clinical nutrition product	0.25	1	0.27±0.006	2
Meal replacement product 1	0.71	1	0.67±0.03	4
Meal replacement product 2	0.43	1	0.49±0.09	2

n = Number of replicate analyses.

Advantages of Dynamic Bandpass Tuning in Dynamic Reaction Cell ICP-MS

John Latino, Ken Neubauer, and *Ruth E. Wolf, PerkinElmer Instruments, Shelton, CT 06484 USA
Gordon Wallace, PerkinElmer Instruments, Norcross, GA USA
Maryanne Thomsen, PerkinElmer Instruments, Ltd., Seer Green, UK

ABSTRACT

This paper discusses the advantages of Dynamic Bandpass Tuning (DBT) which, in conjunction with chemical resolution, eliminates interfering species in the analysis of complex matrices by ICP-MS. The use of an active quadrupole inside the dynamic reaction cell allows a mass bandpass window with both low-mass and high-mass cutoff regions to be established. This mass bandpass window is tunable and changes appropriately with the analyte mass being passed through the analyzer quadrupole. Because undesirable product ions can be expelled from the reaction cell, highly reactive gases that provide superior interference reduction such as ammonia, oxygen, and methane can be used.

INTRODUCTION

The development of ICP-MS instruments with gas-filled cells between the plasma and analyzer quadrupole has shown great promise in reducing polyatomic interferences. There are currently several cell-based ICP-MS systems available on the market and trying to distinguish between them can be a difficult and confusing task. Although these instruments appear similar on the surface, they differ greatly in their ability to eliminate interferences. This paper will take a brief look at what types of systems are available and discuss how they differ before presenting data from the ELAN® Dynamic Reaction Cell™ (DRC™) system (PerkinElmer SCIEX, Concord, Ontario, Canada) that demonstrate its superior performance in removing interferences.

Cell-based ICP-MS instruments can be categorized into two classes, depending on the configuration and operating conditions of the cell. The first type of cell system that was developed was the collision cell system. These systems evolved from the collision cells that were developed in the early 1980s for organic mass spectrometry (e.g., LC-MS systems). The first commercial collision cell ICP-MS was introduced in 1987. In a typical collision cell system (or sometimes called a collision/ reaction cell by those wanting to confuse the issues) a multipole is placed inside an enclosed cell located in the ion path of the instrument. The purpose of the multipole is to keep all the ions focused inside the cell and to funnel them into the analyzer quadrupole – in other words, it acts as an ion guide. The multipole used is typically a hexapole or octopole, as these devices are more efficient as ion focusing devices. In fact, in many designs the multipole collision device actually replaces part of the normal ion lens assembly of a typical non-cell system. Because this type of collision cell system uses a passive (or non-mass filtering) ion-guide in the cell, we can also refer to these systems as passive ion-guide systems in order to avoid further confusion.

Passive ion-guide collision cell systems typically rely on collisional induced dissociation (CID) caused by the collision of the reaction gas molecules with the analyte and inteferent ions inside the cell to reduce some common polyatomic interferences. Typically, collision cells operate under lower pressures and higher ion energies than reaction cells. Because collision cells operate at higher ion energies, some endothermic reactions (i.e., reactions that require energy input) may occur, but these reactions are secondary and are not predictable or controllable[a]. Another point to note is that although the collision cell instruments commercially available for ICP-MS operate at fairly high gas flow rates, this is due to the design of the collision cell and does not indicate the actual pressure inside the cell. In a passive ion-guide system, the only way to attempt to control the collisions and reactions that may occur is to limit the total number of gas molecules present for collision by keeping the pressure in the cell low and limiting the gases used to those that are fairly non-reactive, such as hydrogen or helium.

Dynamic Reaction Cell Systems

The second type of system is a dynamic reaction cell system. Currently only one dynamic reaction cell system is available, the ELAN Dynamic Reaction Cell or DRC. The ELAN DRC has been available commercially since early 1999. A dynamic reaction cell system is one where an active mass-filtering device is placed inside the reaction cell. In the case of the ELAN DRC, an active quadrupole is used inside the cell and is controlled to act as a mass filter. The ELAN DRC eliminates interferences through two mechanisms: chemical resolution and Dynamic Bandpass Tuning (DBT). Chemical resolution uses the chemical reactions between the interfering species and the reaction gas to create products that do not interfere with the analyte of interest. The chemical reactions occur-

*Corresponding author.

[a]*For a more detailed technical discussion, see references (1) and (2).*

ring inside the dynamic reaction cell are between ions that are essentially at thermodynamic equilibrium (also called thermalized ions)[b]. In order to have ions that are thermalized inside a reaction cell, the pressure inside the cell must be relatively high and the energy of the ions relatively low. This results in only predictable exothermic reactions taking place within the cell. As a result, in the ELAN DRC, the chemistry (and it is *chemistry* that occurs, not just collisions) is predictable using gas-phase kinetic and thermodynamic theory and is transferable from instrument to instrument. This is not the case with passive ion-guide collision cell systems, and significant performance variations have been reported from one instrument to another.

Dynamic Bandpass Tuning

Dynamic Bandpass Tuning or DBT uses the application of a precisely controlled bandpass mass filter inside the dynamic reaction cell to exclude and eject undesirable species from the reaction cell, preventing the formation of new interferences. The use of an active quadrupole inside the dynamic reaction cell allows a mass bandpass window with both low-mass and high-mass cutoff regions to be established. This mass bandpass window is tunable and changes appropriately with the analyte mass being passed through to the analyzer quadrupole – hence the term Dynamic Bandpass Tuning. Because undesirable product ions can be expelled from the reaction cell, highly reactive gases, such as ammonia, oxygen, methane, and others, can be used.

The major difference between the active quadrupole configuration used in the ELAN DRC and the passive ion-guide configuration is the ability to deal with the formation of new species created within the cell.The passive ion-guide systems do not have the ability to establish a precise mass bandpass window inside the cell. In fact, these devices are designed purely to transmit all of the ions that are within the cell to the analyzer quadrupole. As a result, most ions (collision products as well as matrix ions) are stable within the collision cell, providing an opportunity for unwanted and uncontrollable reactions and collisions to occur. This leads to the formation of new interferences and causes higher signal backgrounds. Although this is especially true when using highly reactive gases such as ammonia, even simple gases will produce new interferences from the uncontrolled chemistry inside a passive ion-guide collision cell. These new interferences may obscure masses that have traditionally been interference-free in ICP-MS. There have even been reports at recent conferences by users of these systems that the reactions that are occurring are due to impurities in the reaction gas. Because these simple collision cell instruments do not have any means of controlling the collisions/reactions that occur inside the cell, they must limit the gases used to simple gases, such as H_2 or He, which limits somewhat the possibility of additional interferences being formed. However, this results in a great compromise and non-ideal operation because these gases are less effective in the removal of the primary interference, particularly under the conditions used in the passive ion-guide systems. In addition, the passive ion-guide systems must limit the number of reactions/collisions that occur to just a few by maintaining a low pressure inside the cell; otherwise, the rate of formation of new interferences is too high and the resulting analyte signal loss is too great.

The advantage of the ELAN DRC is that the quadrupole inside the cell has well-defined stability regions, which can be easily controlled by the application of the RPq and RPa parameters to adjust the low- and high-mass cutoff regions, thus establishing the DBT parameters. This means that ions outside the low- and high-mass stability boundaries are unstable in the cell and are ejected. The bandpass sets up an electric barrier that allows interferences to leave the analyte stability region, but does not allow any new interferences (from recombination, for example) to enter. This provides an excellent means of completely controlling the chemistry that occurs inside the DRC beyond simply changing the reaction gas used and the gas flow rate. Another advantage of the ELAN DRC is its ability to filter out these unwanted ions so that they have no possibility of reacting to form new ions that might interfere with masses of interest. This means that the reactions eliminating the interfering species can be allowed to continue to completion, efficiently removing the interference, not just reducing it. In contrast, passive ion-guide systems using kinetic energy discrimination can never allow the reactions to go to completion; otherwise they lose analyte sensitivity (2). This is why the level of interference reduction reported on an active quadrupole system like the ELAN DRC can be between 1,000 to 1,000,000 times better than that of passive ion-guide systems (2,6).

The ELAN DRC ICP-MS employs an active quadrupole inside the gas-filled reaction cell, which provides complete control of the chemistry occurring inside the cell. Background reduction is accomplished with the use of various reaction gases to eliminate interfering species through a process called chemical resolution. Additionally, the DBT parameters on the active quadrupole inside the reaction cell are also used to elimi-

[b]*For additional information, see references (2) to (5).*

nate the possibility of forming secondary interferences from reaction by-products. Through chemical resolution and adjustment of the reaction cell bandpass, interfering species are converted to non-interfering species and, more importantly, ejected from the DRC before the ions enter the analyzer quadrupole. This paper shows the advantages of the DRC over passive ion-guide collision/reaction cell instruments for interference removal and demonstrates the effectiveness of the DBT capability to precisely control the chemistry occurring inside the reaction cell. The ELAN DRC system provides complete interference removal and uncompromising performance in any sample matrix.

EXPERIMENTAL

The instrument used was the ELAN DRC ICP-MS equipped with a quartz cyclonic spray chamber and concentric nebulizer. All studies were run using hot plasma conditions (1000 to 1200W RF power). Interference reduction was accomplished using a suitable reaction gas and adjustment of the DBT parameters. By adjusting these parameters using the automated software routines in the ELAN software, the backgrounds from interfering species are minimized while sensitivity for the analytes is maintained. In addition, once the optimum gas flow rates and mass bandpass values are established for a particular application, they can be reproducibly transferred from instrument to instrument or to other laboratories.

The ELAN DRC system was employed to remove the interfering species that prevent the use of the major isotopes of elements such as selenium, calcium, potassium, and iron in determinations made by conventional (non-DRC) ICP-MS. The elimination of interferences affecting Ca, K, and Fe has been previously discussed (6). In this work, ammonia was used as the reaction gas for the determination of vanadium and zinc. Selenium determinations are illustrated using either a hydrogen/argon mixture (5%/95%) or methane (99.999% pure) as the reaction gas. Several different types of samples were analyzed in this work. Vanadium was determined in 1% hydrochloric acid, while zinc was examined in 1% nitric acid. Selenium was determined in both ground water (undiluted) and serum (1:15 dilution).

RESULTS

Elimination of $^{35}Cl^{16}O^+$ Interferences on ^{51}V

The determination of vanadium in a chloride-containing matrix is problematic due to the presence of $^{35}Cl^{16}O^+$, which appears at m/z =51, the same mass as the primary vanadium isotope. The ELAN DRC effectively removes the $^{35}Cl^{16}O^+$ interference by using the proper reaction gas and optimization of the DBT parameters. $^{35}Cl^{16}O^+$ is eliminated by reaction with NH_3, but without the ability to set DBT parameters, new interferences at m/z = 51 (from Cl-NH_x species) can also form. However, in the DRC these potential new interferences are never seen because the DBT parameters prohibit their formation by excluding Cl^+ from the reaction cell.

Evidence of this is presented in Figure 1, which shows a plot of the signal-to-background (S/B) ratio at m/z = 51. The S/B ratio was calculated by dividing the signal from a 1% HCl solution spiked with 1 ppb vanadium by the signal from the unspiked 1% HCl solution. Two things are occurring simultaneously inside the DRC during this experiment. First, the ammonia reaction gas is reacting with the ClO^+ ions, thus removing them. At the same time, the DBT parameters applied to the ELAN DRC eject any Cl^+ species present in the cell. This is illustrated by the graph in Figure 1, showing that the S/B increases by over 100 as the RPq parameter is increased. The RPq parameter controls the low-mass cutoff of the active quadrupole inside the DRC. As the RPq bandpass parameter is increased from 0.1 to 0.8, the low-mass cutoff threshold increases. At an RPq value of 0.65 to 0.7, the low-mass cutoff is high enough to reject Cl^+ (at masses 35 and 37) from the reaction cell, thus prohibiting the formation of new interferences. This increase in S/B ratio with increasing RPq illustrates

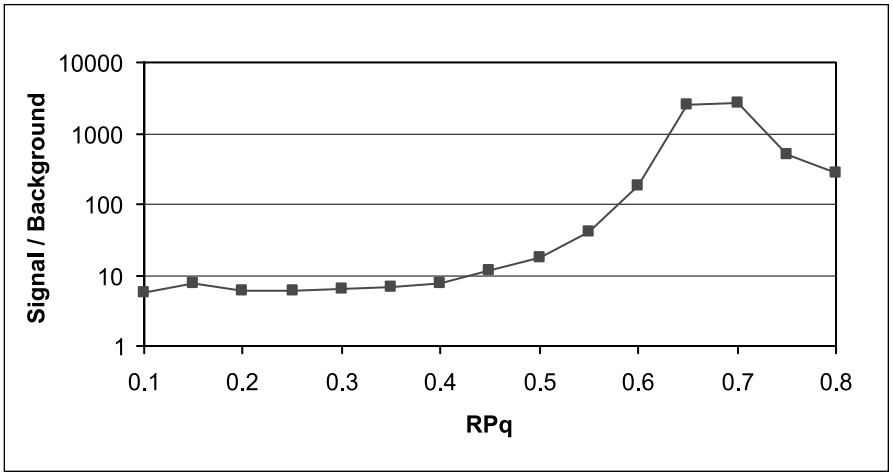

Fig. 1. Effect of RPq on determination of V in a chloride matrix. Plot of m/z = 51 signal for matrix + spike divided by matrix. (Matrix= 1% HCl; Spike=1 ppb vanadium.)

the ability of the RPq parameter to eject both the products from the original interference and any new potential interferences formed with reaction by-products or species in the sample matrix.

In contrast, the S/B values for RPq values below 0.4 are fairly constant, indicating that nearly all of the ions are retained in the cell, allowing the opportunity for reactions to occur and new interferences to form. This is indicative of what would happen inside a passive ion-guide collision cell system. Since this type of system cannot set a low-mass cutoff, all the ions would be retained inside the cell, causing additional interferences and increased background signals.

These experiments demonstrate that optimal interference reduction for the ELAN DRC is obtained with RPq = 0.65 for the determination of V in chloride-containing matrices.

Elimination of Unwanted Reaction By-products

Zinc is often a difficult element to determine in real-world matrices due to the number of different interferences that can affect the various zinc isotopes. While reaction cells can be effective in eliminating the primary interference, it is also important not to generate additional interferences at the same time with reactions that can occur between the sample matrix, the reaction gas, and the original interference components. In other words, it is not enough to just eliminate the primary interference. It is also important, especially with unknown sample matrices, to be able to prevent the formation of new interferences. An example showing the effectiveness of DBT in eliminating potential interferences is seen in Figure 2, which displays four spectra of 10 µg/L zinc, acquired using ammonia as the reaction gas (flow rate = 0.70 mL/min) at two different RPq or bandpass settings. An RPq setting of 0.25 was used to simulate the conditions inside a passive ion-guide collision cell system while an RPq setting of 0.65 was used as the optimized DBT setting on the ELAN DRC. At RPq=0.25 (dashed-line spectrum), $Zn(NH_3)_x$ (x=1-3) clusters form due to reactions within the reaction cell of species from both the reaction gas and the sample matrix. The presence of these clusters obscures the determination of analytes that may be present at these masses, such as Sr, Mo, and Sn, as seen in Figures 2b-2d. However, by increasing RPq to 0.65 (solid-line spectrum) in the DRC, the formation of $Zn(NH_3)_x$ cluster ions does not occur and the trace amounts of Sr and Sn present in the sample can now be seen. This example demonstrates that the dynamic bandpass tuning capabilities of the DRC prevent the formation of new, interfering species within the cell by allowing complete control over the chemistry occurring inside the cell. In contrast, other cell-based systems do not have the ability to apply a mass bandpass inside the cell. As a result, ions from both the reaction gas and, more importantly, the sample matrix can react to form new interferences. This greatly limits the ability of other cell-based systems to remove interferences in real-world sample matrices.

Analysis of Se in Ground Water

Two ground water samples containing high amounts of humic acids were analyzed for selenium. Since the exact matrix composition

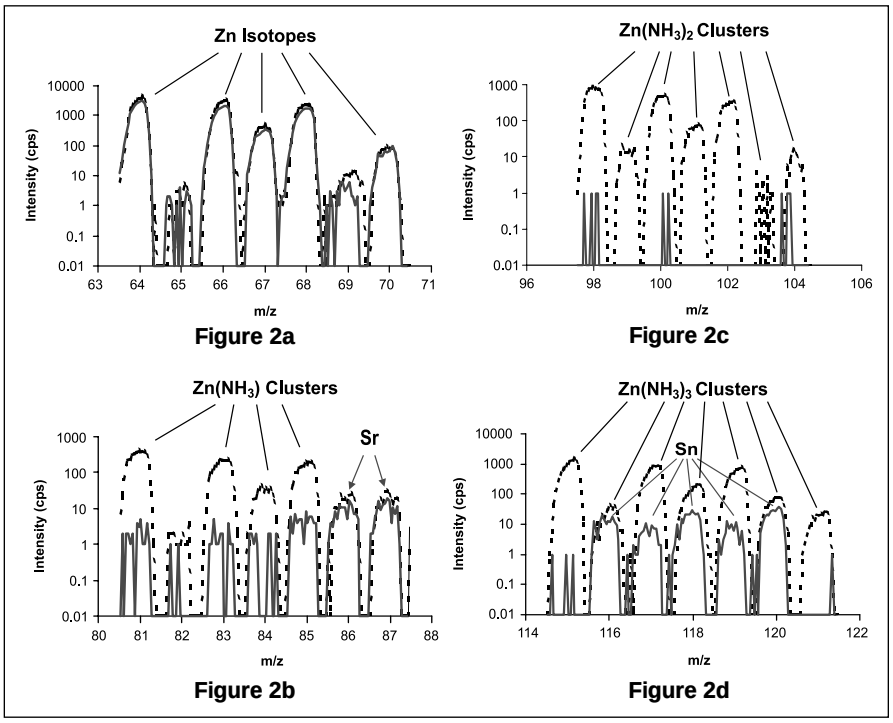

Fig. 2(a-d). Spectra of 10 ppb zinc with RPq=0.25 (dashed-line spectrum) and RPq=0.65 (solid-line spectrum). Sr and Sn are present in trace amounts.
Figure 2a shows the Zn peaks from masses 64 to 70.
Figure 2b shows the mass region from 80-87.
Figure 2c shows the mass region from 97-105.
Figure 2d shows the mass region from 114-121.
Figures 2b, 2c, and 2d illustrate the $Zn(NH_3)_x$ clusters (dashed-line spectrum) that can form without the ability to establish a mass bandpass window inside the reaction cell.

of the samples was unknown, three selenium isotopes were monitored: ^{77}Se, ^{78}Se, and ^{82}Se. Hydrogen (5% H_2 in 95% argon) was used as the reaction gas. ^{80}Se was not monitored for these samples due to regulatory constraints for this particular application. The analysis was first performed with RPq=0.45 in order to simulate the conditions that would typically be present in a passive ion-guide collision cell instrument. This resulted in all three selenium isotopes reading different concentrations, as shown in Table I. The cause of these discrepancies is the complex chemistry occurring inside the cell between the reaction gas and the species in the sample matrix. These chemistries most likely originate from the organic species (i.e., humic acids) present in the samples which decompose in the plasma to their most basic components: C^+, H^+, and O^+. These species enter the collision cell where they can react to form a variety of hydrocarbon species at different masses. These data illustrate that these reactions occur even when a simple reaction gas such as hydrogen is used.

The same samples were analyzed again, but with a DBT parameter of RPq=0.60. At this higher RPq value the low-mass cutoff threshold is raised to eject the unwanted ions from the DRC. This results in the ability to control the chemistry inside the cell by ejecting the matrix species ions before they can react to form new interferences. The results obtained using this higher RPq setting appear in Table II, and show that all three isotopes read virtually the same concentration. This example again illustrates the importance and effectiveness of changing the dynamic bandpass setting on the quadrupole inside the DRC to control the chemistry inside the cell and eliminate interferences in real sample matrices.

TABLE I
Determination of Selenium in Ground Water with RPq=0.45 ("collision-cell" conditions)

Sample	^{77}Se (µg/L)	^{78}Se (µg/L)	^{82}Se (µg/L)
1	127	26.8	10.4
2	131	26.4	9.55

TABLE II
Determination of Selenium in Ground Water with RPq=0.60 (ELAN DRC with DBT)

Sample	^{77}Se (µg/L)	^{78}Se (µg/L)	^{82}Se (µg/L)
1	3.54	4.01	3.02
2	3.54	3.61	2.86

Analysis of Serum

The determination of selenium in serum is important in the clinical field since selenium is an essential nutrient that can also be toxic at elevated levels. Methane was used as the reaction gas in order to remove the argon dimer interference at mass 80, allowing the detection of ^{80}Se. Figure 3a shows a mass spectrum of the selenium region of a Standard Reference Material (SRM) serum containing 4.9 ng/mL Se acquired with RPq=0.4. This low RPq setting simulates what would occur in a passive ion-guide collision cell instrument. The bars overlaid with the spectrum show the natural selenium isotopic abundance, refer-

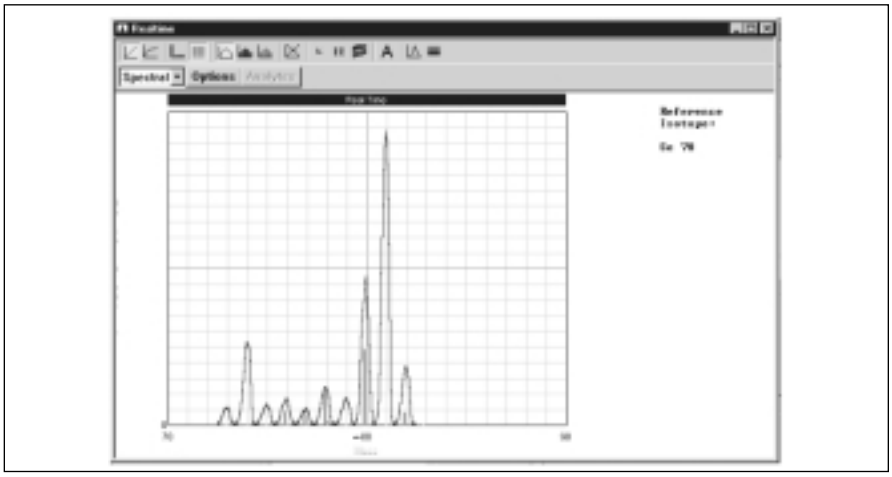

Fig. 3a. RPq = 0.4 ("collision cell" conditions).

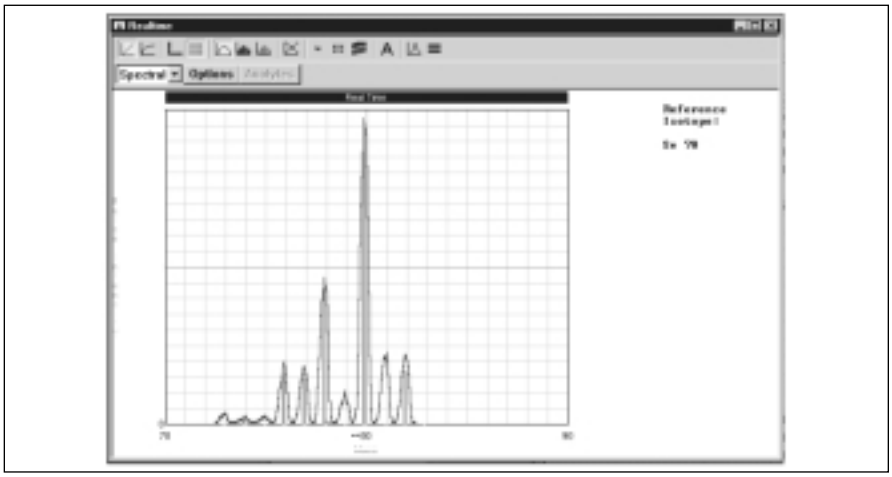

Fig. 3b. RPq = 0.7 (ELAN DRC with DBT conditions).
Figures 3a and b. Effect of the dynamic bandpass tuning parameter RPq on selenium isotopes in Seronorm serum (15x dilution).

enced to $^{78}Se^{+}$. As seen in this figure, the natural isotopic abundance and the observed signals from the Se isotopes do not correspond. The increased signal on some of the Se isotopes is caused by interferences from the organic sample matrix.

However, if we re-analyze the same sample using a DBT parameter of RPq=0.7, the interferences are eliminated, as shown in Figure 3b. This spectrum shows that when using RPq=0.7, the measured and natural isotopic patterns correspond exactly. Again, this example demonstrates the effectiveness of DBT in eliminating interferences – both plasma-based and those formed from the sample matrix.

CONCLUSION

The results of these studies demonstrate the necessity of the Dynamic Bandpass Tuning or DBT function for modifying the transmission characteristics of a reaction cell to completely control the chemistry occurring inside the cell. The data presented compare results obtained under simple collision cell conditions (by using low RPq values to simulate a no-bandpass condition) to those obtained with high RPq values to establish a low-mass cutoff on the quadrupole inside the ELAN DRC system. The data presented show that without a DBT function, all ions entering the cell are stable. These ions can then react with other species inside the cell to form new interferences, resulting in incorrect results. This is particularly true for real sample matrices where the exact composition of the sample may be complex and completely unknown. As a result of the ability of the ELAN DRC system to control the chemistry occurring inside the cell using the DBT function, correct results can be obtained when analyzing complex matrices.

The combination of an active quadrupole inside the ELAN DRC ICP-MS and the ability to use any reaction gas provides the ELAN DRC with two ways of simultaneously eliminating interferences: chemical resolution and DBT. This combination allows the ELAN DRC system to completely control the chemistry occurring inside the reaction cell with any sample matrix and reaction gas. In contrast, collision cell instruments using passive multipole ion-guides inside the cell rely primarily on physical collisions and uncontrollable reactions with impurities in the reaction gases to eliminate interferences (7). Because these ion-guide collision cell systems have no way of rejecting unwanted ions from the cell, they have no way of controlling the chemistry inside the cell. As a result, these passive collision cell instruments must avoid the use of highly reactive gases, such as ammonia, even though these gases provide superior interference reduction. Instead, collision cell instruments must use less reactive gases, such as helium and hydrogen, which reduce, but do not completely eliminate, interferences. Although limiting the gases used can somewhat limit the reactions that can occur, the ability to establish a tunable mass bandpass inside the cell is critical in order to control the reactions that can occur between the reaction gas and species in the sample matrix. This is an important distinction, since in the real world the analyst has no control over the constituents of the sample matrix. The data presented in this paper demonstrate the superiority of the ELAN DRC ICP-MS in eliminating interferences in ICP-MS in any complex matrix.

REFERENCES

1. S. D. Tanner, V.I. Baranov, and D. R. Bandura, "Reaction Chemistry and Collisional Processes in Multipole Devices," in Plasma Source Mass Spectrometry: The New Millennium, eds. J. G. Holland and S. D. Tanner, The Royal Society of Chemistry, Cambridge, pp. 99-116 (2001).
2. Dmitry R. Bandura, Vladimir I. Baranov, and Scott D. Tanner, "Reaction Chemistry and Collisional Processes in Multipole Devices for Resolving Isobaric Interference in ICP-MS," Fresenius' J. Anal. Chem. (2001, article 00869, in press).
3. Vladimir I. Baranov and S. D. Tanner, "A Dynamic Reaction Cell for Inductively Coupled Plasma Mass Spectrometry (ICP-DRC-MS), Part 1: The rf- field energy contribution in thermodynamics of ion-molecule reactions," J. Anal. At. Spectrom. 14, 1133 – 1142 (1993).
4. Scott D. Tanner and Vladimir I. Baranov, "A Dynamic Reaction Cell for Inductively Coupled Plasma Mass Spectrometry (ICP-DRC-MS). II. Reduction of Interferences Produced Within the Cell," J. Am. Soc. Mass Spectrom.10, 1083-1094 (1999).
5. Scott D. Tanner, Vladimir I. Baranov, and Uwe Völlkopf, "A Dynamic Reaction Cell for Inductively Coupled Plasma Mass Spectrometry (ICP-DRC-MS), Part III. Optimization and Analytical Performance," J. Anal. At. Spectrom.15, 1261-1269 (2000).
6. "ELAN DRC ICP-MS System with Dynamic Bandpass Tuning: An Unequalled Approach to Reducing Interferences and Improving Detection Limits," PerkinElmer Instruments, D-6354 (2000).
7. Barry L. Sharp, "Collisions and Reactions for the Masses," paper O-70, European Winter Conference on Plasma Spectrochemistry (February 4-8, 2001, Hafjell, Norway).

On-line Ion Exchange Preconcentration in a Sequential Injection Lab-on-valve Microsystem Incorporating a Renewable Column With ETAAS for the Trace Level Determination of Bismuth in Urine and River Sediment

Jianhua Wang and Elo Harald Hansen*
Department of Chemistry, Technical University of Denmark
Building 207, Kemitorvet, DK-2800 Kgs. Lyngby, Denmark

ABSTRACT

A sequential injection system for on-line ion exchange separation and preconcentration of trace level amounts of metal ions with ensuing detection by electrothermal atomic absorption spectrometry (ETAAS) is described. Based on the use of a renewable microcolumn incorporated within an integrated lab-on-valve microsystem, the column is initially loaded with a defined volume of beads of an SP Sephadex C-25 cation exchange resin. After having been exposed to a metered amount of sample solution, the loaded bead suspension is precisely manipulated within the valve to allow reproducible elution of the retained analyte by 30 µL nitric acid (1:16,v/v) which, via air segmentation, are then transported into the graphite tube for quantification. The content of the used column is afterwards discarded and new column material is aspirated for the next run. The ETAAS determination is performed in parallel with the preconcentration process of the ensuing sample. The performance of the system is demonstrated for the determination of bismuth. With 2.4-mL sample loading, an enrichment factor of 33.4, a detection limit of 27 ng L^{-1}, along with a sampling frequency of 10 h^{-1} was obtained. The relative standard deviation was 2.3% for the determination of 2.0 mg L^{-1} Bi (n = 7). The procedure was validated by determination of bismuth in a certified reference material CRM 320 (river sediment) and by bismuth spike recoveries in two human urine samples.

INTRODUCTION

The determination of low or trace level amounts of metals by electrothermal atomic absorption spectrometry (ETAAS) often requires the use of suitable preconcentration and/or separation procedures in order to attain the necessary sensitivity and selectivity.

Such schemes are advantageously executed in flow injection (FI) or sequential injection (SI) systems which, in addition to reducing sample and reagent consumption, allow all manipulations to be made on-line under enclosed and strictly controlled conditions, thereby minimizing the risk of contamination from the environment.

Various separation/preconcentration procedures have been suggested and applied, such as liquid-liquid extraction (1), (co)precipitation (including the use of knotted reactors) (2-4), adsorption (5,6), hydride generation (7), or ion exchange (8-10). The latter is possibly the most versatile and used approach, relying on incorporating small column reactors containing suitable resin materials into the FI/SI-system. However, ion exchange column reactors suffer from some inherent drawbacks. First is the volume change that many ion exchange resins undergo when they are converted from one form to another, i.e., from the acidic to basic form. If a micro column, therefore, is exclusively subjected to a unidirectional flow, the ensuing swelling or shrinking of the resin will cause a progressively tighter packing and, hence, increased flow resistance, leading to impaired performance or even resulting in blocking of the flow (11,12). This can be alleviated by using countercurrent flow during the loading and elution sequences, but similar problems may arise over extended periods of operation. The second problem is that the surface properties of the resin might be irreversibly changed after having been subjected to a large number of samples, either due to contamination, deactivation, or even loss of functional groups (13). These problems are especially serious when using ETAAS as the detection device, because the limited accommodation volume of the graphite tube requires that the retained analyte must be eluted completely (or at least to a reproducible degree) within a very small volume of eluent. Irregularities might consequently lead to risks of carryover in long-term operations.

All of these problems might be readily overcome by using an approach where the ion exchange material is discarded and renewed after each measuring cycle. Such a system was recently proposed by the present authors using the so-called lab-on-valve system (9,14) which in its design only consumes very minute amounts of ion exchange material. The cost per assay is amply compensated for by superior performance. In fact, two approaches are conceivable: (a) The analyte-loaded ion exchange beads are transported directly into the graphite tube where they are pyrolized and the analyte is atomized and quantified (9) or (b) the loaded beads can be eluted and the eluate forwarded to the ETAAS instrument for measurement (14). Both approaches have been tested with satisfactory results, although the latter appears to yield the lowest RSD values.

*Corresponding author.

Atomic Spectroscopy
Vol. 22(3), May/June 2001

In the present communication, the applicability of the novel format encompassing elution and renewal of the resin material is communicated and demonstrated for the assay of low levels of bismuth. Precise and accurate analytical methods for this potentially toxic element are in great demand because bismuth increasingly has found use in the production of pharmaceuticals and cosmetics (15). Furthermore, assay of bismuth is of interest in biological and environmental samples where the presence of interfering matrix constituents ordinarily might cause severe signal depression (16) and deteriorate the detection limit (17).

EXPERIMENTAL

Instrumentation

A PerkinElmer AAnalyst™ 600 atomic absorption spectrometer, equipped with Zeeman background corrector, AS-800 autosampler, and THGA™ graphite furnace, was used. The bismuth hollow cathode lamp (S&J Juniper & Co.) was operated at 25 mA, using a wavelength of 232.0 nm and a spectral bandpass 0.2 nm. Pyrolytically coated graphite tubes (PerkinElmer, part No. B3 000641) were employed. Integrated absorbance with a read time of 3 s was used for evaluating the results. The ETAAS was coupled with a FIAlab-3500 flow injection/ sequential injection system (Alitea, USA), equipped with an external 6-port selection valve (SV) mounted with an integrated "lab-on-valve" microsystem (14), syringe pump (SP, 2.5 mL), and auxiliary peristaltic pump. The syringe pump and valve were controlled by a separate computer, independent of the spectrometer. As detailed previously (3), the computer for the ETAAS was made a "slave" of the computer of the FIAlab-3500, whereby all unit operations could be effectively synchronized. Zeeman background correction was used for all measurements.

The "heart" of the system, that is, the integrated micro conduit is shown in Figure 1. Mounted vertically on a selection valve, the conduit is manufactured by Perspex (diameter 50 mm, thickness 10 mm), and contains 7 micro channels (i.d. 1.66 mm, length 12.0 mm), drilled to correspond with the orifice of the selector in the center. Two of the channels (port 4 and the central port) served as micro columns for accommodating the ion exchange bead resin material (details are given in Figure 2 and below). Small pieces of PEEK tubing (i.d. 1.60 mm, length 3.5 mm) with an internal channel (17.8 µm) were inserted into these two channels in order to hold the beads within the cavities of the micro columns and preventing them from escaping. Other characteristics of the "lab-on-valve" system have been previously described in detail (9).

All externally used tubes shown in Figure 1 were made of PTFE. The holding coil (HC) was made from 141.5 cm (i.d/o.d = 1.50 mm/2.10 mm) tubing, corresponding to 2.5 mL. The line from HC to the micro column in the central port was made from (i.d/o.d = 0.50 mm/1.70 mm) tubing. The delivery tube from port 4 to the graphite tube (VG

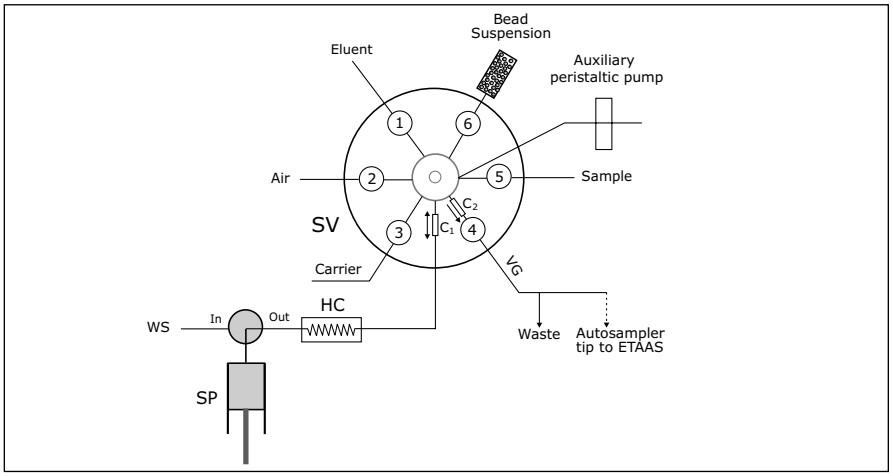

Fig. 1. Manifold for the sequential bead injection-elution on-line ion exchange preconcentration. SV = 6-port selection valve mounted with the integrated micro conduit; SP = syringe pump; HC = holding coil; C_1, C_2 = micro columns within the lab-on-valve micro system; VG = communicating tube between the micro conduit and the ETAAS.

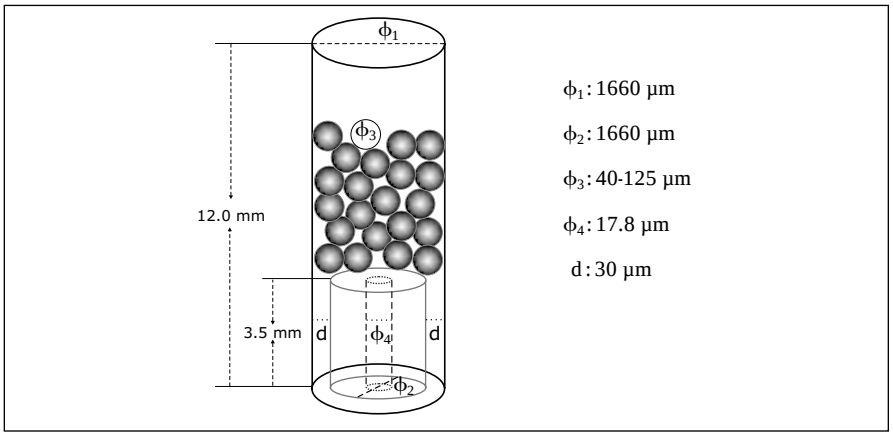

Fig. 2. Schematic diagram of the micro column.

line), which was inserted into the arm of the autosampler, was made from (i.d/o.d = 0.50 mm/1.60 mm) tubing, the length being 30 cm, corresponding to 60 µL.

Reagents

All reagents used were of analytical grade or better, and Milli-Q™ water was used throughout. Working standard solutions of bismuth were obtained by step-wise dilution of a 1000-mg L^{-1} standard solution (PerkinElmer) with a 0.10 M acetate buffer of pH 3.7. The cation exchange resin, SP Sephadex™ C-25 (Amersham Pharmacia Biotech AB, dry bead size: 40-125 µm, Na^+ form), was converted to the H^+ and K^+ forms, as described previously (9), and suspended in an appropriate amount of Milli-Q water. The practical suspensions used in these experiments were 1:10-1:20 (w/v).

Other chemicals used were: HNO_3 (65%, Merck), $HClO_4$ (70%, Merck), HF (40%, Merck), acetic acid glacial (100%, Merck), and potassium acetate (BDH).

Samples and Sample Pretreatment

River Sediment

Community Bureau of Reference (BCR) CRM-320 (river sediment): 0.1 g of CRM 320 was weighed and transferred to a PTFE beaker to which 3.0 mL of 65% nitric acid and 2.5 mL of 40% HF were added. The sample was soaked for 1 hour, then heated gently on a hot plate until fumes appeared and the solution had nearly dried. After cooling, 1.0 mL of perchloric acid was added. The content was heated to near dryness and 5.0 mL of Milli-Q water added; heating continued to near dryness again. The content was dissolved in 0.10 M acetate buffer solution (pH 3.7) by gentle heating and diluting to 100 mL with the buffer. As the content of iron in the final digestion solution greatly exceeds the tolerable limit, and since it is not possible to dilute further in order to maintain the bismuth content within the measuring range, the majority of the iron was eliminated by extraction with ether.

Urine Samples

A 20-mL urine sample was transferred into a PTFE beaker and 15 mL of 65% nitric acid was added. The mixture was heated gently on a hot plate to near dryness. After cooling, 1.0 mL of perchloric acid was added and the solution again heated to near dryness. Then 5.0 mL of Milli-Q water was added and heated to near dryness. The content was dissolved in 0.1 M acetate buffer solution (pH 3.7) and diluted to 50 mL with the buffer. A further 10-fold dilution was performed before actual assay in order to alleviate any matrix effects from dissolved salts.

Operating Procedure

The FIA/SIA-system used is shown in Figure 1. The cation exchange bead suspension is first aspirated into a 1.0-mL plastic syringe, which is mounted vertically on port 6 of the valve. Operation is not initiated until the beads have settled on the bottom of the syringe. At the same time, the whole system is conditioned by making SP aspirate 2000 µL washing solution (0.02% nitric acid), which is subsequently propelled forward through port 4 to waste.

Port 5 has two lines, which are connected to the sample solution and the auxiliary peristaltic pump, respectively. On changing sample, the pump is started to aspirate the sample solution past the central flow-through port, whereupon it is stopped.

A separation/preconcentration cycle runs through four steps, which are as follows:

Step 1: Preconditioning.
SP is set to aspirate 600 µL of the carrier solution through port 3 (flow rate 150 µL s^{-1}), 550 µL of which is directed subsequently via the central port to port 4 (100 µL s^{-1}) to rinse the micro column C2 and the VG line. 50 µL of carrier solution is thus left in the holding coil.

Step 2: Preconcentration.
The central port is directed to port 5, and 2400 µL of sample solution is aspirated (150 µL s^{-1}) and stored in HC. Thereafter, 15 µL of bead suspension is very slowly (3 µL s^{-1}) aspirated into column C1 through port 6. The central port is now directed to port 4 and while SP moves slowly forward (12 µL s^{-1}), the beads are transported to column C_2 along with the sample solution, that is, the preconcentration is taking place. The 50 µL of the previously stored carrier solution is also propelled to wash the column after the preconcentration. 500 µL carrier and 480 µL air are then aspirated into HC through port 3 and port 2, respectively, at a flow rate of 100 µL s^{-1}. 240 µL air is afterwards propelled through port 4 (24 µL s^{-1}), thereby leaving the carrier solution in HC, 60 µL of air in the VG line, and 240 µL of air between the holding coil and the central port. At the same time, the ETAAS program is activated.

Step 3: Eluting the beads and transporting the eluate to the furnace.
30 µL of nitric acid (1:16, v/v) is aspirated through port 1 into C_1 (5 µl s^{-1}). Afterwards, the central port is directed to port 4, and SP is directed to move slowly forward (8 µl s^{-1}), whereby the analyte-loaded micro column C_2 is eluted and the eluate, sandwiched by air, is transported into the graphite tube via the autosampler tip.

Step 4: Discarding the used beads and returning to the preconditioning step.
In this step, advantage is taken of the fact that the resin beads are soft and therefore, at high flow rates, can become squeezed and can pass through the narrow exit channel of

Atomic Spectroscopy
Vol. 22(3), May/June 2001

column C_2 (14). Thus, with the central port still in the position of port 4, and after the autosampler tip has moved out of the graphite tube, SP is set to move forward to propel the previously aspirated carrier solution at a flow rate of 100 µL s^{-1}, whereby all the beads in C_2 are flushed out and directed to waste. At the same time the VG line is rinsed.

The ETAAS program was set up so that when one sample was processed in the FIA/SIA system, the previously handled sample was quantified in the furnace.

RESULTS AND DISCUSSION

ETAAS Parameters

The effects of the pyrolysis and the atomization temperatures were investigated thoroughly and the results are shown in Figures 3 and 4. These studies showed that at a pyrolysis temperature lower than 250ºC, unacceptably high background signals were obtained. Well-shaped and maximum signals were obtained at a pyrolysis temperature around 400ºC and by fixing the atomization temperature at 1200ºC. At higher pyrolysis temperatures, bismuth tended to be lost, i.e., about 20% was lost at 600 ºC and 85% at 800 ºC. Furthermore, by increasing the holding time from 10 to 40 s, the background was decreased and the analyte signal enhanced. A pyrolysis temperature of 400ºC, along with a holding time of 40 s, was therefore used.

The experimental results also showed that the integrated absorbance value increased when the atomization temperature was increased from 900 to 1200ºC, the analyte peak being broadened at lower atomization temperatures, i.e., lower than 1000ºC. Therefore, only results recorded above 1100ºC are given in Figure 4. The signal reached maximum at about 1200ºC and changed merely marginally within the 1100-1300ºC range, yielding well-shaped peaks. Further increases in the atomization temperature led to significantly decreasing integrated absorbance values, i.e., at 1500ºC the integrated absorbance dropped to only about 60% of the value at 1200ºC. As a compromise, an atomization temperature at 1200ºC was chosen. The temperature program for the graphite furnace is summarized in Table I.

TABLE I
Graphite Furnace Program for the Determination of Bismuth

Steps	Temperature (ºC)	Ramp (s)	Hold (s)	Argon flow rate (mL min^{-1})
Preheating	70	5	10	250
Drying	130	5	20	250
Pyrolysis	400	20	40	250
Atomization	1200	0	3	0
Cleaning	2500	1	2	250

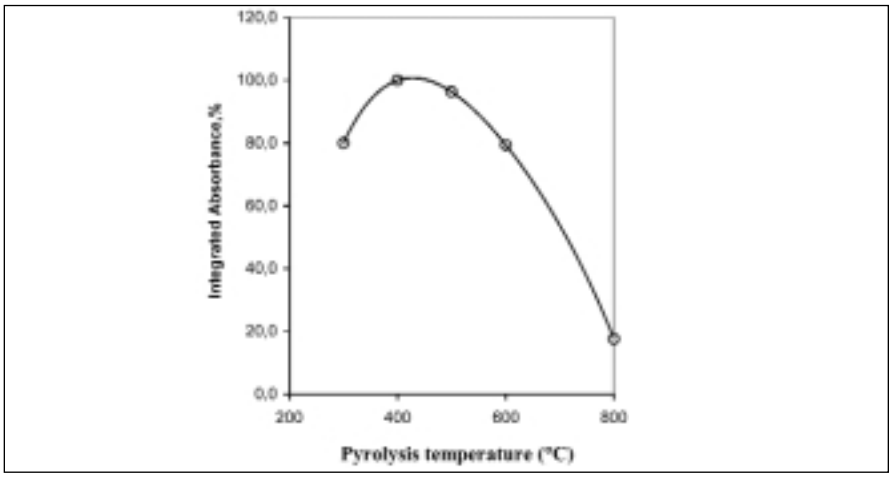

Fig. 3. Effects of pyrolysis temperature as recorded at the following conditions: 2.0 µg L^{-1} Bi^{3+}; sample flow rate 12 µL s^{-1}; buffer pH 3.7; sample loading time 200 s; holding time 40 s; and atomization temperature 1200ºC.

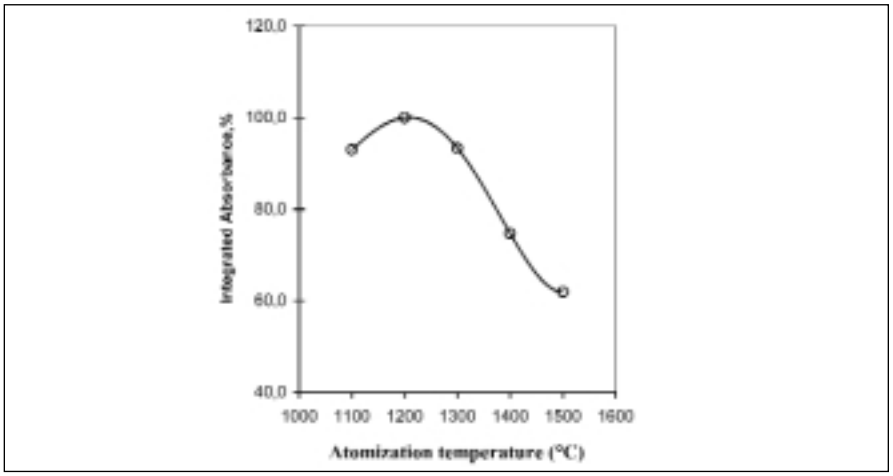

Fig. 4. Effects of atomization temperature as obtained at the following conditions: 2.0 µg L^{-1} Bi^{3+}; sample flow rate 12 µL s^{-1}; buffer pH 3.7; sample loading time, 200 s; pyrolysis temperature 400ºC; and holding time 40 s.

It is interesting to note that both the pyrolysis and atomization temperatures are lower than the recommended values (18). This might be attributed to the fact that no chemical modifiers were used in the present study.

Effects of Acidity and Ion Exchanger Forms

Studies of the effects of sample acidity showed that the enrichment efficiency of bismuth was optimal within a pH range of 3.0-4.8, using either the H^+ form or the K^+ form of the SP Sephadex C-25 resin. Furthermore, both forms yielded approximately similar enrichment efficiencies. The blank level for the K^+ form resin, however, was found to be about 0.05-0.06 integrated absorbance, which is much higher than that for the H^+ form resin, which gave values around 0.01 integrated absorbance. The H^+ form of the SP Sephadex C-25 resin was therefore used in the ensuing experiments, and the acidity of the sample was controlled by using a 0.10 M acetic acid-potassium acetate buffer solution at pH 3.7.

Effects of Eluent Concentration and Its Corresponding Volume

Nitric acid was used as the eluent since the present preconcentration procedure is aimed to be used later in conjunction with ICP-MS. Figures 5 and 6 show the effects of the concentration and the volume of the eluent, respectively. It is obvious from Figure 5 that the integrated absorbance increased rapidly when increasing the concentration of nitric acid up to 6.25% (1:16 v/v), but a further increase in the acidity resulted in very limited signal enhancement. It can also be seen from Figure 6 that by flowing 30 µL of 6.25% nitric acid through the micro column, the majority of the retained bismuth can be eluted (ca. 85%). Considering that the furnace can only safely accommodate this volume in one operative step, very little is gained by eluting the last 15%, because this would require a total of 50-60 µL of eluent.

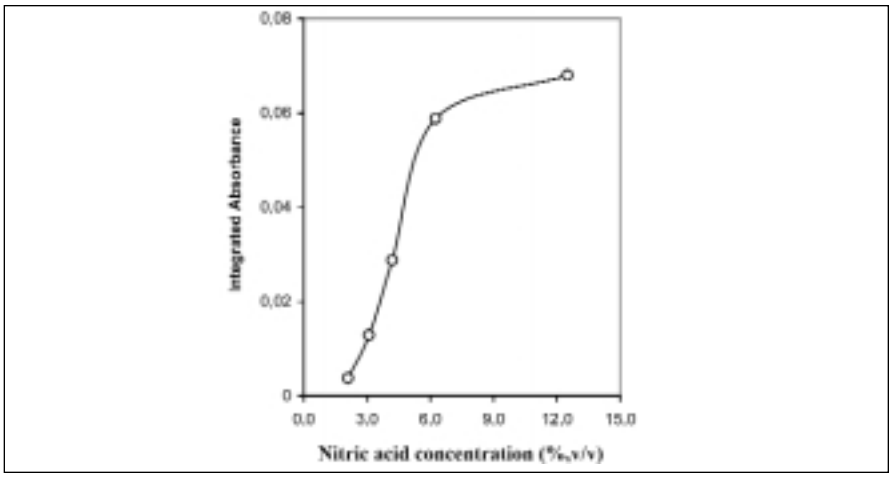

Fig. 5. Effects of eluent (nitric acid) concentration obtained at the following conditions: 2.0 µg L^{-1} Bi^{3+}; sample flow rate 12 µL s^{-1}; buffer pH 3.7; sample loading time 200 s; pyrolysis temperature 400ºC; and atomization temperature 1200ºC.

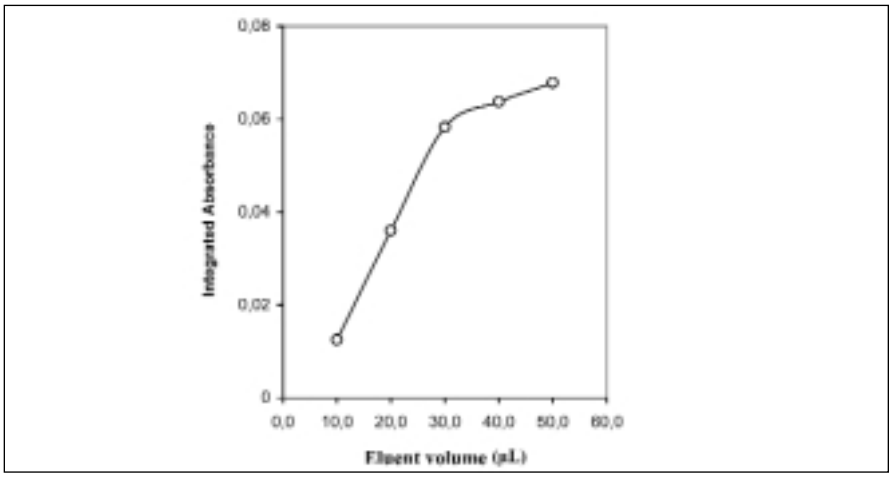

Fig. 6. Effects of eluent (nitric acid) volume obtained at the following conditions: 2.0 µg L^{-1} Bi^{3+}; sample flow rate 12 µL s^{-1}; buffer pH 3.7; sample loading time 200 s; pyrolysis temperature 400ºC; and atomization temperature 1200ºC.

Effects of Sample Loading Time, Sample Flow Rate, and Eluent Flow Rate

The experiments showed that the enrichment factor of bismuth increased linearly with increasing sample loading time. No breakthrough was observed by loading 2.4 mL sample within the concentration range of 0.10-3.0 µg L^{-1}. The sample loading time was fixed at 200 s, corresponding to 2.4 mL of sample, as a compromise between the sampling frequency and the enrichment efficiency.

It is very critical to control the sample flow rate within a certain range in order to obtain the optimal enrichment efficiency. The results indicated that the enrichment factor increased with the sample flow rate within a range of 4-12 µL s^{-1}, which is in contrast to the previous study for nickel preconcentration, where the enrichment efficiency was improved by decreasing the sample flow rate within the same

range (14). At higher flow rates, a slow decline in the enrichment factor was observed; yet at sample flow rates exceeding 30 µL s^{-1}, a very rapid drop was recorded. This is attributed to the fact that at high flow rates, the beads tend to become squeezed and lost via the space between the inner wall of the channel and the small piece of PEEK tubing. A sample flow rate of 12 µL s^{-1} was therefore chosen throughout.

The investigations on the effect of eluent flow rate indicated that the enrichment factor of bismuth was increased by decreasing the eluent flow rate, although the gain is not significant within the range of 4-16 µL s^{-1}. A substantial decrease of the signal was observed at higher flow rates exceeding 30 µL s^{-1} (loss of beads, as indicated above). An eluent flow rate of 8 µL s^{-1} was adopted for further studies.

Interferences

The potential interferences from substances or ions that might often be encountered in biological and environmental samples were studied.

The results showed that at a bismuth concentration level of 2.0 µg L^{-1}, and within a ±5% error range, 1.0 mg L^{-1} Co^{2+}, Cd^{2+}, and Mn^{2+}; 5.0 mg L^{-1} Cu^{2+}; 10.0 mg L^{-1} Zn^{2+}, Fe^{3+} and Pb^{2+} do not interfere with the determination of bismuth. The common matrix cations, such as Na^{+}, Ca^{2+}, and Mg^{2+} do not interfere up to a level of 2.3 g L^{-1}, 200 mg L^{-1}, and 120 mg L^{-1}, respectively. For most biological and environmental samples, the content of coexisting heavy metals will not exceed the concentration levels listed here; therefore, in most cases, no masking agent are actually needed.

Performance of Procedure

The characteristic performance data for the sequential bead injection on-line ion exchange preconcentration procedure for bismuth are presented in Table II. An enrichment factor of 33.4 was obtained in comparison with direct introduction of 20 µL sample solution into the graphite tube.

The procedure was validated by the analysis of a certified reference material (CRM 320, river sediment) and two human urine samples. The recovery tests for the urine samples were made by spiking the original sample solutions with 2.0 µg L^{-1} bismuth before digestion. The digest of the CRM 320 mentioned in the sample pretreatment section was determined directly, and the urine digests were further diluted by a factor of 10 before actual analysis. The results are listed in Table III.

CONCLUSION

On-line ion exchange separation and preconcentration, as facilitated by a sequential injection lab-on-valve micro system incorporating a renewable column, is demonstrated for the determination of low levels of bismuth with detection by ETAAS. As the ion exchange beads of the micro column can be renewed and discarded at will (after one or possibly several runs), the problems associated with long-term operations of conventional ion exchange columns can be effectively eliminated. Even when renewing the column for each sample cycle, the consumption of ion exchange material is minimal. This novel approach therefore promises to possess unique advantages in practical assays. As for the actual assay of bismuth, the detection limit obtained is one of the lowest encountered in the literature (6, 19-21).

TABLE II
Characteristic Performance for the SI Bead Injection On-line Ion Exchange Preconcentration for Bismuth

Linear calibration range	0.05-3.0 µg L^{-1}
Regression equation	$AA = 0.0698C_{Bi} - 0.0008$
Correlation coefficient	r = 0.9996
Sampling frequency	10 h^{-1}
Detection limit (3σ, n=7)	27 ng L^{-1}
Precision (R.S.D, n=7)	2.3 % (2.0 µg L^{-1})
Sample consumption	2.4 mL
Bead consumption	15 µL
Enrichment factor[a]	33.4

[a]The enrichment factor was obtained by comparing with direct introduction of 20 µL sample solution into the graphite tube.

TABLE III
Determination of Bismuth in CRM 320 Certified Reference Material and Human Urine Samples (n=3)

Sample	Indicative Value (µg g^{-1})	Found Value (µg g^{-1})	Spiked (µg L^{-1})	Recovery (%)
CRM 320	0.2 ± 0.5	0.29 ± 0.06		
Urine A[a]		1.04 ± 0.41	2.00	103.0
Urine B[a]		1.43 ± 0.34	2.00	96.3

The results were obtained at 95% confidence level.
[a] in µg L^{-1}.

ACKNOWLEDGMENT

The authors are indebted to the Carlsberg Foundation (Denmark) for providing funds for the acquisition of the ETAAS instrument. Thanks are also due to the Technical University of Denmark for a Ph.D. stipend to one of the authors (JW).

Received March 28, 2001.

REFERENCES

1. J. H. Wang and E. H. Hansen, Anal.Lett. 33, 2747 (2000).
2. Z. L. Fang and L. P. Dong, J. Anal. At. Spectrom. 7, 439 (1992).
3. S. C. Nielsen and E. H. Hansen, Anal. Chim. Acta 422, 47 (2000).
4. J. L. Burguera, M. Burguera, C. Rondon, M. R. Brunetto, and Y .P. Penña, Talanta 52, 27 (2000).
5. Z. R. Xu, S. L. Xu, and Z. L. Fang, At. Spectrosc. 21(1), 17 (2000).
6. E. Ivanova, X. Yan, and F. Adams, Anal. Chim. Acta 354, 7 (1997).
7. J. F. Tyson, R. I. Ellis, S. A. McIntosh, and C. P. Hanna, J. Anal. At. Spectrom. 13, 17 (1998).
8. S. Olsen, L. C. R. Pessenda, J. Ruzicka, and E. H. Hansen, Analyst 108, 905 (1983).
9. J. H. Wang and E. H. Hansen, Anal. Chim. Acta 424, 223 (2000).
10. M. S. Jiménez and J. R. Castillo, J. Anal. At. Spectrom. 12, 1397 (1997).
11. J. Ruzicka and E. H. Hansen, Flow Injection Analysis, 2nd edition, John Wiley & Sons, pp.206 (1988).
12. Z. L. Fang, J. Ruzicka, and E. H. Hansen, Anal. Chim. Acta 164, 23 (1984).
13. J. Ruzicka and L. Scampavia, Anal. Chem. 71, 257A (1999).
14. J. H. Wang and E. H. Hansen, Anal. Chim. Acta 435(2), 331 (2001).
15. B. J. Marshall, Am. J. Gastroenterol 86(1), 16 (1991).
16. S. Toklioglu, S. Kartal, and L. Elci, Mikrochim. Acta 127, 281 (1997).
17. J. S. Chen, H. Berndt, and G. Tölg, Fresenius' J. Anal. Chem. 334, 526 (1992).
18. The THGA Graphite Furnace: Techniques and Recommended Conditions, Manual B 3210.10, Ver.1.2, Bodenseewerk PerkinElmer GmbH (1995).
19. H. O. Haug and Y. P. Liao, Fresenius' J. Anal. Chem. 356, 435 (1996).
20. J. Murphy, G. Schlemmer, I. L. Shuttler, P. Jones, and S. J. Hill, J. Anal. At. Spectrom. 14, 1539 (1999).
21. J. B. B.Silva, M. B. O.Giacomelli, and A. J. Curtius, Analyst 124, 1249 (1999).

Lead Determination in Ultra Micro Samples of Animal Diet Using Graphite Furnace Atomic Absorption Spectrometry

Ivo Iavicoli, Nicolò Castellino, and Giovanni Carelli
Institute of Occupational Health, School of Medicine, Università Cattolica del Sacro Cuore
Largo Francesco Vito, 1-00168 Rome, Italy
Gerhard Schlemmer*
PerkinElmer Bodenseewerk, Alte Nußdorfer Str. 21, D-88662 Überlingen, Germany

ABSTRACT

A graphite furnace atomic absorption spectrometry method has been developed for the determination of very low levels of Pb in small samples of animal diet. The method is based on a microwave-assisted pressure vessel digestion using miniaturized vessels for sample masses of 100 mg. Due to the small acid volume, the dilution factor during digestion was only 10. Detection limits of 5 µg/kg Pb were achieved in a complex matrix consisting of mainly caseine 22% (w/w), corn starch 28.6%, sucrose 30%, cellulose 4%, soya oil 7%, minerals 5.2%, vitamins 2%, and DL methionine 0.4%. The reproducibility of the method was 15% at a Pb concentration of 37 µg/kg and 11%, respectively, using the standard additions method before and after digestion. The recoveries of Pb added to the samples prior to or after digestion were 83.2 ± 3.0% and 82.3 ± 2.2%, respectively.

INTRODUCTION

Lead (Pb) is a ubiquitous element, which for centuries has been known to have toxic effects on human health. Thus it is among the elements of interest in the fields of toxicology, industrial hygiene, food and environmental health sciences. Due to Pb monitoring efforts during the last decades, the exposure levels to this metal both in the general environment and in the workplace underwent a significant decline. However, the reduction of adverse effects on health due to high Pb levels did not address low-level Pb effects as was shown by recent studies performed for children (1-3). Reports on low-level Pb concentrations, though rare in the literature, show signs of disturbances in iron and lipid metabolism in rats (4).

For these reasons, we examined the effects of low Pb levels in animal diet (4000 µg/kg down to < 40 µg/kg) in mice to ascertain not only the disappearance of health effects related to an excessive intake of Pb, but eventually the appearance of other health effects due to Pb depletion. As our research is still in progress, the complete set of analytical results, such as Pb levels in organs and tissues, is not yet available and will be published elsewhere.

In this paper, the development of an analytical method for the determination of Pb in a purified diet prepared for mice is described. This semisynthetic Pb-depleted diet was manufactured specifically for our research and was used to characterize unusually low Pb levels. Zeeman-effect electrothermal atomization atomic absorption spectrometry (Z-ETA-AAS) was used for Pb quantification after digestion of the sample in a microwave-heated pressurized vessel with a mixture of concentrated nitric acid and hydrogen peroxyde. Since certified reference materials for this type of matrix are not available, the analytical quality of the method was tested by addition of known amounts of Pb to 100-mg aliquots of the animal diet before and after digestion of the samples.

*Corresponding author.

EXPERIMENTAL

Reagents

Doubly deionized water was used throughout this study obtained from two deionization systems connected in series (Nuovo RD 30 Elettracqua, Italy and Milli-Q™, system, Millipore, USA). Ultrapure concentrated HNO_3 (69-70% Baker Instra-Analyzed) and H_2O_2 (30%, w/w, Erbatron, Carlo Erba, Italy) were used for preparation of the standards and for digestion of the samples. A 1000-mg/L Pb standard stock solution [$Pb(NO_3)_2$, Plasma Chem Corp, USA] was diluted with 2% (w/v) HNO_3 to obtain a working stock standard of 4 mg/L. In order to match the acidity of the standards and samples, the working stock standard was further diluted with 20% (v/v) HNO_3 to obtain 20 µg/L and 40 µg/L working standards. Additions to the samples were made with standards in 0.2% HNO_3, respectively.

The chemical modifier was obtained by diluting 30 µL of a 10-g/L Mg solution and 50 µL of a 10-g/L Pd solution (PerkinElmer modifier solution) to 1 mL with deionized water. A deposition onto the platform of 10 µL modifier corresponded to 3 µg of Mg (as nitrate) and 5 µg of Pd (as nitrate).

Digestion of Diet

The animal diet was manufacutured and supplied by Altromil (Germany) as cylindrical chips with an average weight of 1.7 g/chip. The main matrix components were caseine 22% (w/w), corn starch 28.6%, sucrose 30%, cellulose 4%, soya oil 7%, minerals 5.2%, vitamins 2%, and DL methionine 0.4%. Per each kg of animal diet, macroelements such as calcium (9.5 g), phosphorus (6.5%), magnesium (0.7%), sodium (2.5%,), and potassium (5.3 %) as well as oligoelements such as iron (170 mg), manganese (100 mg), zinc (25 mg), copper (5 mg), iodine (1 mg), cobalt (0.4 mg), Mo (0.1 mg), fluorine (4.2 mg), and selenium (0.2

mg) were added. Storage and handling of the chips required special care to avoid contamination by environmental Pb. Therefore, polyethylene bags were used as the chip containers. Disposable plastic gloves, precleaned stainless steel ladles, etc., were used for handling of the chips and transferring them to the cages, etc. Approximately 50 g of the animal diet was finely milled using a grinder equipped with titanium blades. Seven aliquots of the powder were accurately weighed on a micro balance (Mettler, Mod. AT 20, Switzerland, resolution ± 0.002 mg) within a very narrow mass range of 100.41 ± 0.16 mg and introduced separately into seven 7-mL Teflon® vessels containing each 0.4 mL HNO_3 and 0.1 mL H_2O_2. For recovery measurements, another set of 10 animal diet samples with an average weight of 100.41±0.16 mg was prepared and 10 µL of a solution of 4.0 mg Pb/L in 1% (v/v) HNO_3 was added to five of the samples. The Pb addition corresponded to 40 ng Pb/vessel. In both sets of experiments, two blanks of the oxidants, 0.4 mL HNO_3 and 0.1 mL H_2O_2, were run.

After sealing with a torque wrench, the vessels were introduced into larger Teflon vessels (120 mL) and digestion was carried out in a MDS-2000 microwave oven (CEM Corporation, Matthews, NC, USA). The microwave program consisted of two steps at 80°C and 120 C°, respectively. Microwave power at 20% and 100%, respectively, was required to reach these temperatures at 100% fan speed. The total run time was 10 minutes for step 1 and 15 minutes for step 2.

After cooling, the vessels were opened and the blanks and digests diluted with water in acid-decontaminated 1-mL graduated flasks (Duran NS 7/16, Hirschmann Techcolor, Germany). The recovery studies were performed by diluting 0.2 mL of the unspiked digests with 0.2 mL 0.2% HNO_3 or 0.2 mL of a solution of 40 µg/L Pb in 0.2% HNO_3. The solutions were then made up to 1-mL volume with deionized water. All Pb determinations were calibrated against the two Pb working standards.

Determination of Lead in the Animal Diet Samples

All determinations were performed on a PerkinElmer Model 4100ZL atomic absorption spectrometer, equipped with longitudinal Zeeman-effect background correction and transversely heated graphite atomizer (THGA™). End-capped pyrolytically coated tubes (part no. B3000652) were used throughout the study. A PerkinElmer Lumina™ hollow cathode lamp was used at the recommended primary resonance wavelength of 283.3 nm and a spectral bandpass of 0.7 nm. The integrated absorbance (8 s integration time) was evaluated. Standard, samples, and spikes were injected onto the integrated platform at room temperature. A 20-µL sample and 10 µL of the modifier were injected with the PerkinElmer Model AS-70 autosampler.

The drying, ashing, and atomization temperatures were selected after the usual optimization using pyrolysis and atomization curves (see Figures 1). The final furnace time/temperature program is listed in Table I.

RESULTS AND DISCUSSION

The ashing and atomization study (see Figure 1) shows that losses of Pb in the Pb standards in 20% HNO_3 without modifier already occur at temperatures as low as 500°C. The same applies to the pyrolysis curve obtained in the animal diet digest run without using a modifier. However, very subtle differences in the maximum pyrolysis temperature can be observed.

From a theoretical point of view, it should be expected that the integrated absorbance of Pb in the reference solutions and in the digested samples stays constant up to the pyrolysis temperature where the first Pb losses are encountered. The integrated absorbances in this range should be identical for sample and reference solutions. However, this was not the case. While the sensitivity of the acidified standard at temperatures close to 500°C is about 10% higher than in the sample, Pb losses already occur at temperatures above 500°C. The Pb sensitivity in the samples still increases with pyrolysis temperatures up to 700°C and falls abruptly at temperatures higher than 700°C. A Pb stabilization by the matrix, which consists mainly of phosphate, magnesium, and calcium, is not unexpected. The slightly lower Pb sensitivity in the sample at lower pyrolysis temperatures cannot be explained. The amount of Mg, Ca, and PO_4^{3-} added

TABLE I
Optimized Graphite Furnace Time/Temperature Program

Step #	Temp. (°C)	Ramp (s)	Hold (s)	Gas Flow (mL/min)
1	130	1	30	250 Ar
2	160	5	20	250 Ar
3	650	5	25	250 O_2
4	650	1	20	250 Ar
5	800	1	25	250 Ar
6*	1800	0	6*	0
7	2400	1	3	250 Ar

* Read active in step 6.

Atomic Spectroscopy
Vol. 22(3), May/June 2001

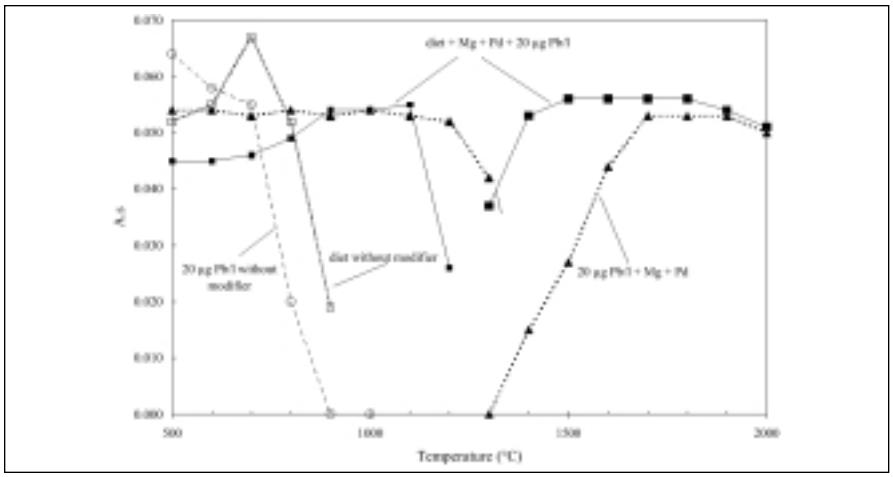

Fig. 1. Pyrolysis and atomization curves for Pb in 20% HNO_3 and in the digested animal diet samples without and with 3 µg of Mg (as nitrate) and 5 µg of Pd (as nitrate) modifier.

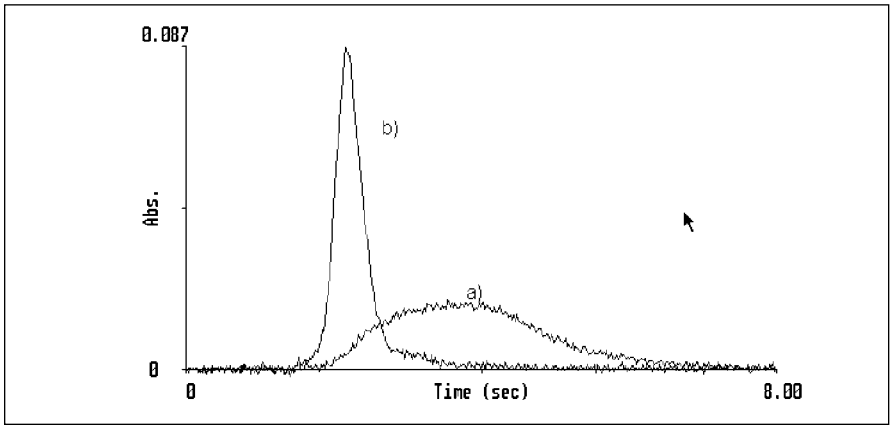

Fig. 2. Time-resolved graphics of (a) 20 µg/L Pb reference solution and (b) digested animal diet with 20 µg/L Pb added. New graphite tube used. Atomization temperature 1800°C. Integrated absorbance A_Q of (a): 0.048 s; of (b): 0.044 s.

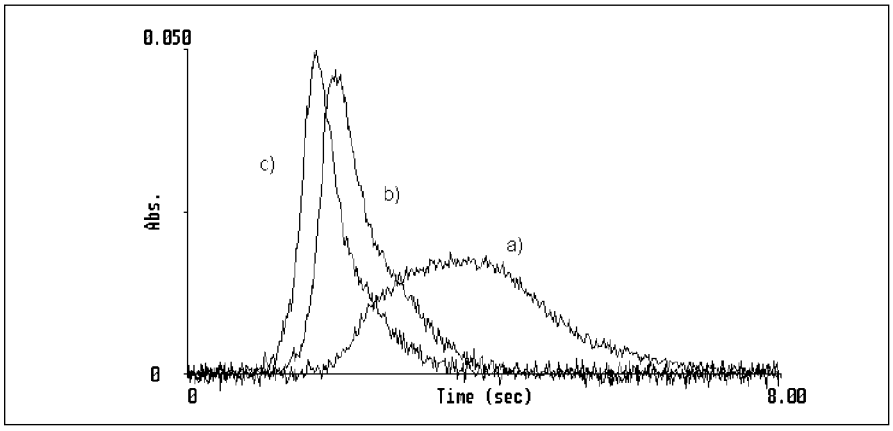

Fig. 3. Influence of matrix on peak shape. 20 µg/L Pb reference solution. (a) cycle 12; A_Q = 0.056s, (b) cycle 47; A_Q = 0.044s, (c) cycle 64; A_Q = 0.037s. Acid standards and samples were run in sequence.

with each sample injection corresponds to 3 µg, 45 µg, and 95 µg, respectively, and is certainly within or even above the range of typical modifier additions.

As expected, addition of the Pd/Mg modifier both to standard and sample results in a substantial improvement of the Pb thermal stability (see Figure 1). The modifier thermally stabilizes Pb in acidified standard solutions up to a pyrolysis temperature of about 1100°C. The Pb sensitivity in the sample matrix is identical to the standard solutions between 900°C and 1100°C and stable within this range. At lower pyrolysis temperatures, the integrated absorbance of equal amounts of Pb is again about 10% lower than in the standard solutions. The modifier shifts both the maximal pyrolysis temperature and optimal atomization temperature to higher values. While optimal sensitivity is obtained at temperatures higher than 1700°C in acidified Pb solutions, the analyte is completely released from the sample matrix at 1400°C. This effect was reported in the literature (5) and was also confirmed in the present study as can clearly be seen from the shapes of the time-resolved absorbance in the acidified standard and sample (see Figure 2).

It should be pointed out that this effect depends on the age of the graphite tube. The appearance time of 0.4 ng of Pb standard prepared in 20% HNO_3 and atomized at 1800°C was 1.8 s after 12 firings. The peak shifted to 1.3 s and to 1.1 s after 47 and 64 firings, respectively. Apart from the early shift, the peak becomes much sharper and the maximum is shifted left (see Figure 3). No shift in appearance time or peak shape was observed after 64 firings. It has to be pointed out that the reference solutions and animal diet digests were run in sequence in this experiment. The change in appearance time and peak shape

has certainly been partially caused by the carbonaceous and matrix-rich sample.

The appearance time of Pb in the sample or of Pb added to the sample is always earlier than in the reference solution but is affected by tube ageing to a much lesser degree. It was 1.4 s after six firings and 1.1 s after 18 and 64 cycles. The peak maximum still shows some early shift between peak 18 and 64 (see Figure 4). No difference in peak shape between sample and Pb added to the sample could be found.

After about 60 firings, the performance of a new graphite tube showed a pronounced decline, i.e., the characteristic mass increased by 15%, from, e.g., 33 pg to 38 pg for standards. However, a higher characteristic mass (about 17%) was observed throughout the tube lifetime for Pb added to the samples. The very broad shape of the Pb standard (Figure 2) at the beginning of the tube lifetime required an atomization time as high as 8 s, which is obviously unnecessary for routine determinations. In fact, the Pb addition performed at regular intervals, e.g., every five samples, will correct perfectly for the slow increase in characteristic mass in the span of the tube lifetime. This will assure measurement accuracy and keep the time for the determinations reasonably short.

The relatively short long-term stability is probably related to factors such as high sample load, strong oxidizing power of the high concentration of oxidizing acids in the sample, and the use of oxygen during the pyrolysis step. Even if the digestion procedure reduced the amount of organic polymeric substances such as proteins and starch substantially, a 20-µL injection of sample corresponded to 1 mg animal diet. We did not analyze the digest, but a high content of monosaccharides (amino acids and their nitro derivatives) as well mineral components (predominantly calcium phosphate) has to be expected. The initial very high concentration of nitric acid and hydrogen peroxide is certainly reduced during the digestion process, but is probably still significantly higher than under standard conditions.

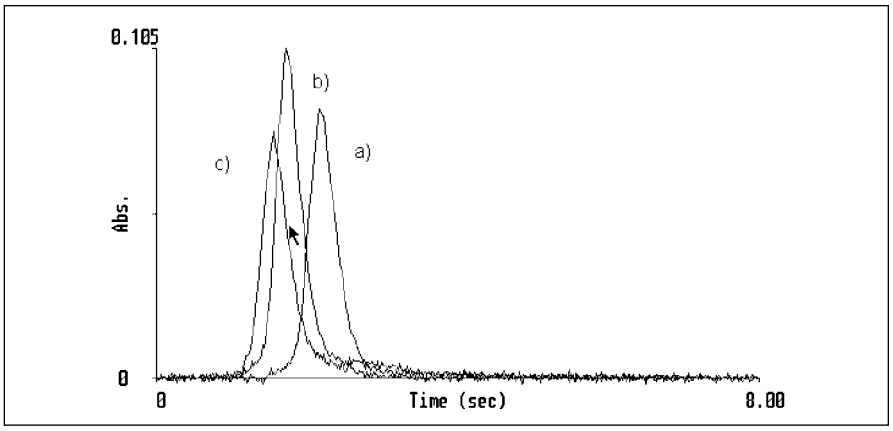

Fig. 4. Influence of matrix on peak shape. Diet with 20 µg/L Pb added. (a) cycle 6; A_Q = 0.044s, (b) cycle 18; A_Q = 0.052s, (c) cycle 64; A_Q = 0.038s. Acid standards and samples were run in sequence.

It has to be pointed out that this method has been specifically optimized for the determination of low levels of Pb in micro amounts of samples. The resulting high matrix concentrations impose an unusually high demand on background correction and stability of the graphite tube surface.

Table II shows the within- and between-run precision. The results are based on seven individually digested samples, each analyzed 10 times by the method of standard additions. The Pb additions were performed by the autosampler directly onto the platform. The average percent standard deviation of both samples and additions (n = 70 each) was 4.2 and 1.7% (data not shown).

TABLE II
Within- and Between-Run Precision and Recovery (Additions were made to seven 100-mg wet-ashed animal diet samples. Each sample and addition was analyzed 10 times and standard deviations refer to the mean result of each sample. Recoveries are based on calibration with acidified reference solutions.)

Digest #	Weight sample (mg)	Within- and between*-run precision (µg/kg) (Mean ± SD, n = 10 each digest)	Average recovery (%)
1	100.56	42 ± 2	83.3
2	100.49	40 ± 3	80.5
3	100.29	33 ± 1	85.3
4	100.22	31 ± 1	84.5
5	100.26	41 ± 2	87.5
7	100.27	41 ± 3	78.5
8	100.55	34 ± 2	82.5
Mean ± SD	100.38 ± 0.14	37 ± 5*	83.2 ± 3.0

Table III illustrates the same statistical evaluations with the difference that Pb additions were made before digestion. Five samples and five additions were digested and the Pb concentration was determined in this experiment.

The relative standard deviation of the samples was 15% or 11%, respectively, for Pb concentrations as low as 35-37 µg/kg in the solid animal diet. The additions were made directly onto the platform prior to or after digestion. No background compensation errors similar to those observed by Parsons (6) were observed at the Pb levels investigated. The Pb level of the animal diet was found to be 37 ± 5 µg/kg if calibrated with the method of standard additions. No significant statistical difference between recoveries was found when additions were made prior to or after digestion with values of 83.2 ± 3.0% and 82.3 ± 2.2% for the two sets of data. The detection limit, based on the dry solid sample, was found to be about 5 µg/kg based on three times the standard deviation of the blank.

CONCLUSION

The method reported is the methodical solution to the determination of extremely low Pb concentrations in very limited sample amounts of biological origin. The chemical composition of the matrix, type, and concentration of the acids used and the pyrolysis conditions considered optimal for these types of samples resulted in a limited graphite tube lifetime. Nevertheless, the analytical procedure was successfully used in the measurement of the Pb concentration in a matrix which requires Pb levels to be quantitated and which is very demanding for graphite furnace AAS. The method has also been used to study and to avoid Pb contamination in the course of animal feeding and caging.

Received June 25, 2001.

TABLE III
Within- and Between-Run Precision and Recovery
(Additions were made to five animal diet samples prior to digestion. Each sample and addition was analyzed in triplicate and standard deviations refer to the mean result of each sample. Recoveries are based on calibration with acidified reference solutions.)

Digest #	Sample amount (mg)	Within- and between*-run precision (µg/kg) (Mean ± SD, n = 3 each digest)	Average recovery (%)
1	100.56	41 ± 3	83.4
2*	100.49		
3	100.29	31 ± 2	82.0
4*	100.22		
5	100.26	31 ± 2	79.4
6*	100.59		
7	100.27	36 ± 2	85.4
8*	100.56		
9	100.56	37 ± 3	81.5
10*	100.26		
Mean ± SD	100.41 ± 0.16	35 ± 4*	82.3 ± 2.2

REFERENCES

1. A.M. Bernard, A. Vyskocil, H. Roels, J. Kritz, M. Kodl, and R. Lauwerys, Environ. Res. 68, 91-95, (1995).
2. E. Emory, R. Pattillo, E. Archibold, M. Bayorh, and F. Sung. Am. J. Obstet. Gynecol. 181, 2-11, (1999).
3. T. Sakai, Ind. Health 38, 127-142 (2000).
4. Reichlmayr-Lais and M. Kirchgessner Lead in: "Handbook of nutritionally essential minerals," pp 479-492. Boyd L. O'Dell, Roger A. Suncle. Library of Congress, USA (1997).
5. G. Schlemmer and B. Radziuk , "Analytical Graphite Furnace Atomic Absorption Spectrometry, A Laboratory Guide," p. 132; Birkhäuser Verlag, Basel, Boston, Berlin (1999).
6. Y.Y. Zong, P.J. Parsons, and W. Slavin, Spectrochim. Acta B 53, 1031-1039 (1998).

Optimized Conditions and Analytical Performance for the Determination of Cu in Serum and Urine Samples Using a Single GFAAS Procedure

Agostinho A. Almeida* and José L.F.C. Lima
CEQUP/Departamento de Química-Física, Faculdade de Farmácia, Universidade do Porto
Rua Aníbal Cunha, 164, 4050 Porto, Portugal

ABSTRACT

The determination of copper in biological samples is of major importance in clinical chemistry and very often, especially when Wilson's disease is suspected, the simultaneous analysis of both serum and urine is necessary. Therefore, a single analytical procedure with proven reliability in the simultaneous determination of copper in both matrices becomes of great practical interest for clinical laboratories.

This work describes the optimization and evaluation of a Zeeman-effect background correction GFAAS method. It differs only in the prior dilution of the serum samples (1+24) and allows the determination of copper in both serum and urine samples with proven accuracy, precision, and robustness.

The method provides a limit of detection of 0.98 µg/L, a limit of quantification of 3.3 µg/L, and a characteristic mass of about 23 pg. Repeatability (%RSD) was 1.3% for a standard solution (20 µg/L), 2.4% for urine (26 µg/L), and 1.4% for serum (29 µg/L) samples. Between-run and between-day reproducibility was typically better than 5%. Accuracy has been assessed using the standard additions method/calibration curves slope ratio, which was 1.057 for serum and 1.023 for urine, and by the analysis of commercial control samples. Additional evaluation of the results obtained in the determination of copper in serum was made by comparison with Flame AAS analysis.

INTRODUCTION

Copper is a well-established essential trace element required for the catalytic activity of numerous metalloenzymes involved in the biological processes, such as iron metabolism, elastin, collagen and keratin crosslinking, catecholamines and hemoglobin synthesis, free radical detoxification, and normal oxidative metabolism (1-5). Under normal conditions, dietary copper is absorbed through the intestinal mucosa at a rate ranging from 50 to 80% (2) and is transported to the liver, bound to albumin, by portal circulation. Once in the liver, copper is redistributed over several metalloproteins, namely ceruloplasmin, through which it is excreted to the plasma and reaches concentrations of 700 - 1400 µg/L in man, 800 - 1550 µg/L in woman (1). The main route of copper excretion is in bile and other intestinal fluids. In effect, the total amount excreted every day through faeces normally equals the total dietary intake, the urinary excretion being very low (less than 50 µg/day) (1,4).

There are several pathologies related to copper metabolism, the most important being the well-known Wilson's disease, a disease of autosomal recessive inheritance in which the biliary excretion of copper and its incorporation into ceruloplasmin are both severely impaired, resulting in an excessive deposition of copper in the liver, brain, cornea, and kidneys (1-5). In clinical chemistry, the determination of copper is generally required to support the diagnosis of this disease and involves copper determination in both serum and urine samples (2). Wilson's disease is characterized by abnormal low levels of copper in serum (1,4) and results in an increased renal excretion (1,4), thus facilitating the differential diagnosis towards other hypocupremia conditions.

Although there are some colorimetric methods described for the determination of copper in serum (2), laboratories prefer to use Flame AAS (1,2,4,5) due to its specificity, speed of analysis and easy utilization, in addition to normal copper levels being within its analytical capabilities regarding sensitivity. The same does not occur in the determination of urinary copper, because typical concentration levels (less than 50 µg/L, as referred before) require the use of GFAAS (5). This is extensively discussed in the literature where Flame AAS is used for the determination of copper in serum (or plasma) (6-15) and GFAAS for the determination of copper in urine (16-19). Therefore, laboratories must have two instrumental techniques (often requiring two different pieces of equipment) to perform these determinations.

In order to overcome this problem, several approaches enabling urinary copper determination by Flame AAS have been tried, namely prior extraction or on-line preconcentration procedures (20-23), determination by the standard additions method (24), and instrumental arrangements to increase sensitivity (25). Nevertheless, these proposals present several disadvantages and/or are not completely satisfactory regarding sensitivity improvement, and thus GFAAS is still the selected technique for this analytical purpose.

Another alternative consists in using only GFAAS for the determination of both urinary copper and serum copper. Several authors (26-30) reported the determination of copper in serum by GFAAS, but only a few (31,32) intended to develop a single analytical procedure that would be simultaneously suitable for both types of matrices.

**Corresponding author.*

One of the methodological proposals (31) dates back to the early years of GFAAS, which might justify its re-evaluation considering the analytical capabilities of present instrumentation and the latest concepts in GFAAS, namely the stabilized temperature platform furnace (STPF) concept (33). Moreover, although the instrumental conditions used (including the graphite furnace program) were the same for both matrices, the results were obtained by reference to a different calibration curve depending on the sample under analysis: aqueous standard solutions for urine and a reference serum for serum samples. Another proposed methodology (32), much more recent, aimed at the attainment of a very short temperature program (30 s per determination), which was successfully accomplished. However, under these conditions, the deterioration of the graphite tubes is very critical (34). For economical reasons, there is no interest in reducing the tube's lifetime to obtain a high sample throughput, since even large laboratories generally have very few requests for the determination of copper in serum and urine.

This work describes the optimization of the analytical conditions and the evaluation of the analytical performance of a single GFAAS procedure (same instrumental/furnace conditions and same calibration curve) for the determination of copper in both serum and urine samples. STPF conditions, a set of instrumental and operational parameters considered prerequisite for accurate and precise GFAAS analysis (34), were used. Differing only in terms of the previous dilution required for the serum samples (1+24), the present procedure proved to be precise, accurate, and sufficiently robust for routine laboratory practice.

EXPERIMENTAL

Instrumentation

GFAAS determinations were carried out with a PerkinElmer Model 4100 ZL atomic absorption spectrometer, equipped with a longitudinal Zeeman-effect background corrector, an AS 70 autosampler, and a transversely heated atomizer (THGA™) with end-capped graphite tubes (PerkinElmer Part No. B300-0644). The instrumental parameters and the graphite furnace temperature/time program used are presented in Table I.

For validation of the copper determination in serum, Flame AAS analysis was performed with a PerkinElmer Model 3100 atomic absorption spectrometer, operated according to the manufacturer's recommendations. A hollow cathode lamp (S&J Juniper, Essex, UK) was used as the radiation source for both instruments.

Reagents, Samples, and Standard Solutions

The calibration solutions were prepared by adequate dilution of a 1000-mg/L Spectrosol (BDH, Poole, UK) stock solution. The matrix modifier solution was prepared from magnesium nitrate and palladium nitrate commercial solutions suitable for GFAAS analysis (Merck, Darmstadt, Germany). High-purity water (resistivity >18 MΩ.cm) was obtained in a Milli-Q™ system (Millipore, Bedford, MA, USA). Triton® X-100, pro analysis glycerol and Suprapur nitric acid (Merck) were also used.

The urine samples were a 24-h urine collected in plastic vessels, properly cleaned by immersion in diluted (1+4) nitric acid for 24 hours, followed by rinsing with Milli-Q water. After collection, the samples were acidified (0.4% of Suprapur nitric acid) and kept in the refrigerator until analysis. The serum samples were obtained using the routine collection procedure and kept in the refrigerator until analysis.

The accuracy of the procedure was assessed through the analysis of lyophilized control samples (serum and urine) from Seronorm™ (Nycomed Pharma, Oslo, Norway), which were reconstituted according to the manufacturer's instructions with Milli-Q water.

TABLE I
Instrumental Parameters and GFAAS Program for the Determination of Cu in Serum and Urine Samples

Lamp current	10 mA
Wavelength	324.8 nm
Slit with	0.7 nm, low
Background correction	Longitudinal Zeeman effect
Measurement mode	Peak area (A.s)
Integration time	6 s
Injection volume	20 µL
Injection temperature	20 ºC

Furnace Time/Temperature Program

Step	Temp. (ºC)	Ramp (s)	Hold (s)	Argon gas flow (mL min^{-1})
1	110	1	20	250
2	130	5	30	250
3	1200	10	40	250
4	2000	0	5	0 (read)
5	2400	1	5	250

Procedure

Control of Contamination

Class A glassware was used, previously decontaminated by immersion in diluted (1+4) nitric acid for 24 hours, followed by rinsing with Milli-Q water throughout. Gilson® automatic pipettes (Villiers-le-Belle, France) with disposable plastic tips were also used. The autosampler cups of the GFAAS instrument were used without any treatment and disposed after single use.

Copper Determination

Calibrating solutions and urine samples were diluted 1+1 directly in the autosampler cups using a diluting/matrix modifier solution containing 0.1% (v/v) Triton® X-100, 0.03% (p/v) $Mg(NO_3)_2$ and 0.05% (p/v) Pd (also as nitrate). The serum samples were previously diluted 1+24 with Milli-Q water in volumetric flasks and afterwards also (1+1) in the autosampler cups, as referred for the calibrating solutions and urine samples. All solutions were then analyzed under the conditions presented in Table I and the copper concentration obtained by interpolation in the calibration curve.

RESULTS AND DISCUSSION

Graphite Furnace Program

The method development was focused on the optimization of the graphite furnace temperature/time program. Beginning with the conditions recommended for copper measurements by the instrument manufacturer, the optimal temperatures for the pyrolysis and atomization steps were assessed for standard solutions and for urine and serum samples using the recommended criteria (35). The drying step was defined by visual inspection of the sample behavior (no spattering and perfect drying at the end of this step) and by the analysis of the repeatability of the results.

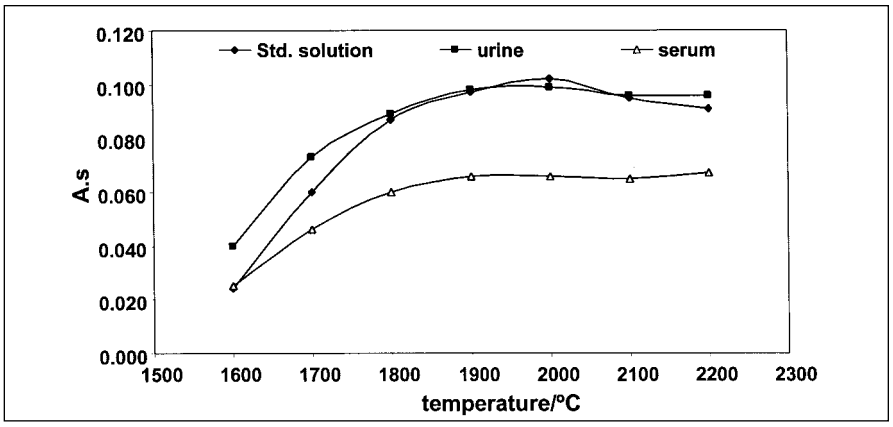

Fig. 1. Relationship between the analytical signal (background-corrected values) and the atomization temperature. Diluting/matrix modifier solution: 0.1% (v/v) Triton X-100, 0.03% (p/v) $Mg(NO_3)_2$ and 0.05% (p/v) Pd. Other conditions as in Table I.

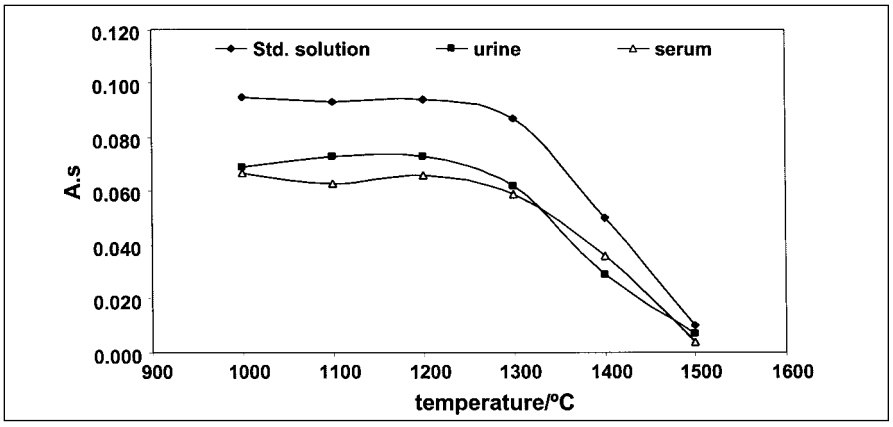

Fig. 2. Relationship between the analytical signal (background-corrected values) and the pyrolysis temperature. Atomization temperature 2000 ºC. Other conditions as in Figure 1.

Figure 1 shows the relationship between the analytical signal (peak area) and the atomization temperature for a standard solution (40 µg/L), a urine sample (spiked to have a similar concentration) and a serum sample, all processed as described before. For all matrices (aqueous standard solution, serum, and urine), the peak area reaches a maximum, and a better peak profile was obtained with a temperature of 2000ºC. The background absorbance also increased with the temperature, though the highest values reached were only 0.140 and 0.097 A.s units for the urine and serum samples, respectively. Therefore, the 2000ºC temperature was selected for the graphite furnace temperature program (Table I). A similar study on the temperature at the pyrolysis step is presented in Figure 2. For the aforementioned matrices, highest atomic absorption signals were found up to 1200ºC and then diminished, when higher pyrolysis temperatures were used. Except for urine, the background signals (Figure 3) were quite stable for pyrolysis temperatures ranging 200 to 1200ºC and always well below the capabilities of the background corrector for the three matrices. However, since removing a corrosive matrix at high tempera-

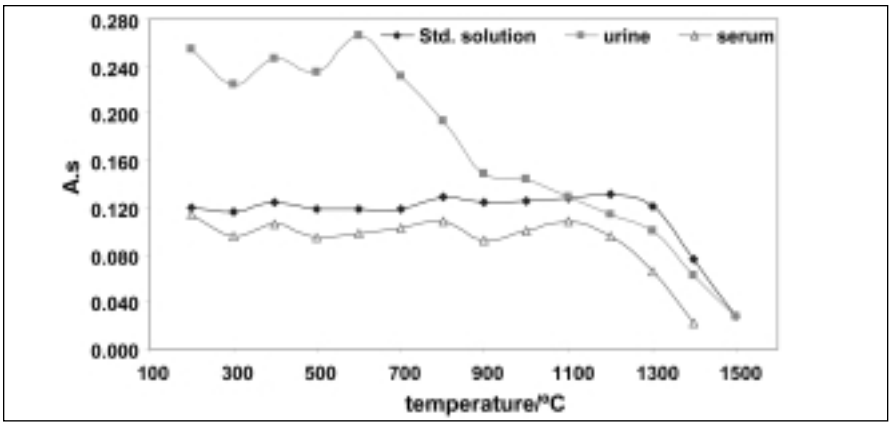

Fig. 3. Relationship between the background signal and the pyrolysis temperature. Same conditions as in Figure 2.

tures (e.g., during atomization) will destroy the graphite tube sooner, the pyrolysis temperature was set to 1200ºC (Table I) to preserve long-term stability (34).

For the other parameters of the program (time and temperature), there was no need to change the values recommended by the manufacturer and those which by default are in the control software of the equipment used.

The results obtained show that a similar behavior can be attained for both sample types as well as for the standard solutions. Therefore, the main purpose of this work can be achieved, i.e., a single graphite furnace time/temperature program for both serum and urine samples and calibration with aqueous standard solutions. It must be stressed that other authors (36) performing the determination of copper in urine and whole blood used a different temperature program for each matrix. In another work on this subject already referred (31) and despite the instrumental conditions used being the same (namely the same graphite furnace program), the urine sample and serum sample atomic absorption signals were referred to different calibrations curves. The disadvantages of both of these works were overcome using the proposed methodology.

Method Validation

The method validation comprised four different aspects: linear response range, precision, accuracy, and limit of detection (LOD) / limit of quantification (LOQ).

Precision was assessed regarding repeatability of replicate injections (n=10) and reproducibility of the results obtained from the replicate analysis of the same serum and urine samples. Reproducibility was evaluated for a set of five urine and five serum samples between two independent determinations on the same day (between-run precision) and between two independent determinations on three consecutive days (between-day precision) (37).

The accuracy of the procedure was evaluated by assessing the parallelism between the calibration curves (CC) and standard additions method (SAM) curves, by analyzing the control samples and, for copper determination in serum, by comparing the results (n=12) with those given for the same samples by a Flame AAS method (14). This consisted in a single dilution of the serum samples (1+1) with deionized water and the preparation of the calibrating solutions with glycerol (10%) to match the viscosity of the samples and standards.

With reference to the LOD, it must be stressed that it is important only for the characterization of the urinary copper determination. Since there are no urine samples without any copper content, the LOD was evaluated by using a blank solution (10 µL of the diluting/matrix modifier solution+10 µL of 0.2% HNO_3). Upon measurement of the signal from 20 consecutive injections, and using the slope of the calibration curve, the LOD was calculated as the concentration corresponding to three times the standard deviation (s) and the LOQ as the concentration corresponding to 10 σ.

Linearity

The relationship between the analytical signal and the concentration was linear up to relatively high copper concentrations, a correlation coefficient of r=0.9996 being obtained for a calibration curve attained with copper standard solutions containing 200, 300, 400, 600, and 800 µg/L. Nevertheless, considering the expected concentration of copper in urine, a calibration up to 100 µg/L is enough and more adequate, because the typical concentrations of urine and serum samples after a 1+24 dilution are within this range. For a total of nine calibration curves, obtained during the precision and accuracy evaluation reported next, there was good linearity within the concentration range of 0 - 100 µg/L, with R^2 values ranging from 0.9982 up to 0.9995 and intercept values from -0.0032 to +0.0023.

Precision

Replicate injections (n=10) of a standard solution containing 40 µg/L (20 µg/L in the injected solution) provided a RSD of 1.3%. Similar values were also obtained for a serum (1.4%) and urine (2.4%) sample with identical concentrations (29 µg/L and 26 µg/L, respectively), verifying good repeatability of the

method. The results in Table II show that in both evaluations (between-run and between-day) reproducibility was acceptable, with a RSD typically less than 5%. The statistical analysis by the paired Student *t*-test at a 95% confidence level showed no significant differences among the set of results obtained every day, which proves that the between-run imprecision is acceptable. Similarly, an ANOVA test proved that the mean values obtained each day were not significantly different (also at a 95% confidence level), thus showing that the analytical between-day imprecision is also acceptable. This robust feature of the method is enhanced by an additional ANOVA test to the six sets of results showing that there were again no statistically significant differences among them.

Accuracy

As referred to above, the accuracy of the analytical procedure was assessed based on the parallelism of the curves obtained by the SAM (for both serum and urine samples) to a CC (standard solutions) (Figure 4). Furthermore, control samples (serum and urine) were analyzed and, particularly in the determination of copper in serum, the results obtained from the analysis of 12 samples by the GFAAS procedure were compared to those provided by a Flame AAS method (14) (see Table III). The results obtained upon the evaluation of accuracy, summarized in Table IV, show that the proposed method may be considered accurate for both the serum copper and urinary copper determinations. As shown in Figure 4, significant matrix effects may be excluded since the slope of the three straight lines is similar; thus validating the use of a calibration with aqueous standards for both determinations of copper in serum and copper in urine. Moreover, the results presented in Table III show that the GFAAS determination of copper in serum provides minor relative errors compared to those obtained by the reference method (Flame AAS). There were no statistically significant differences

TABLE II
Between-run (br) and Between-day (bd) Reproducibility
(Results expressed as µg/L for urine and µg/dL for serum.)

Calibration Curves	Day 1/1	Day 1/2	CV(%) br	Day 2/1	Day 2/2	CV(%) br	Day 3/1	Day 3/2	RSD(%) br	RSD(%) bd
S	0.001856	0.001692		0.001958	0.001952		0.001784	0.001760		
b	-0.0032	-0.0014		+0.0023	+0.0020		+0.0013	+0.0012		
R^2	0.9982	0.9989		0.9990	0.9990		0.9985	0.9995		
Urine samples										
U1	31.2	31.2	0.0	32.1	32.5	0.8	32.0	34.0	4.3	2.7
U2	28.3	27.2	2.8	27.4	27.6	0.6	28.2	27.4	2.0	0.5
U3	22.8	24.9	6.2	25.0	5.4	1.1	25.4	25.4	0.0	3.4
U4	20.2	20.8	2.2	21.4	22.1	2.4	20.7	20.1	2.1	3.6
U5	62.2	62.5	0.3	65.3	68.0	2.9	70.0	68.3	1.8	5.2
Serum samples										
S1	124.4	127.1	1.5	121.1	120.1	0.6	122.6	121.5	0.7	2.2
S2	109.9	108.8	0.7	105.3	105.7	0.3	108.6	108.3	0.2	1.8
S3	108.5	107.2	0.9	101.6	104.2	1.8	104.2	104.2	0.0	2.4
S4	129.9	125.5	2.4	120.1	119.6	0.3	126.5	136.0	5.1	4.6
S5	103.6	104.8	0.8	108.6	107.6	0.7	102.4	103.3	0.7	2.6
	t-test: *t* calculated: 0.16344 *t* critical: 2.26216			*t*-test: *t* calculated: -1.21135 *t* critical: 2.26216			*t*-test: *t* calculated: -0.77918 *t* critical: 2.26216			
	ANOVA test for the mean values of each day: *F* calculated = 0.00267; *F* critical = 3.35413 ANOVA test for all values: *F* calculated = 0.00259; *F* critical = 3.38607									

between both sets of results (see Table IV). The analysis of the reference samples enhances these conclusions, because the results obtained in both determinations (serum and urine) match the values indicated by the laboratories responsible for the certification of those samples.

Sensitivity, LOD, and LOQ

As is usual in GFAAS analysis, the sensitivity depends on the condition of the graphite tube. Using a new graphite tube (end-capped type) enabled calibration straight lines with slopes of about 0.0027 (see Figure 4). However, this initial higher sensitivity tended to decrease very quickly corresponding to the deterioration of the tube end-caps; thus, the slopes of the calibration straight lines reached lower values. These remained quite stable throughout the continuous use of the tubes. Considering nine calibration curves obtained for five consecutive days, totalling over 400 cycles of analyses of standard solutions, urine and serum samples, a mean slope value of 0.0018 was obtained with a standard deviation of 0.0002. For this mean slope value of the calibration curves, the LOD and LOQ were 0.98 µg/L and 3.3 µg/L, respectively.

Other Factors of Analytical Variability

Regarding routine laboratory practice, stability of the standard solutions over a week's work was assessed. Therefore, the solutions prepared on the first day were kept (during the day at room temperature and overnight in the refrigerator) until the last day. Afterwards, their concentration was determined by reference to a calibration curve obtained with standard solutions freshly prepared. Relative errors were less than ±5% (mean value of -3.4%) and thus, for practical purposes, the non-daily preparation of the standard solutions is acceptable.

TABLE III
Comparison of Results (µg/dL) Obtained in the Determination of Cu in Serum Samples by GFAAS and Flame AAS

Sample	Flame AAS[a]	GFAAS[b]	RE (%)[c]
1	125.1	122.5	-2.1
2	107.4	107.4	0.0
3	99.7	104.3	+4.6
4	119.7	122.9	+2.8
5	100.7	105.8	+5.0
6[d]	130.6	130.3	-0.2
7	98.5	104.5	+6.0
8	145.0	145.7	+0.5
9	148.3	153.6	+3.6
10	112.9	119.6	+5.9
11	76.4	74.3	-2.8
12	78.6	75.5	-4.0

[a]Mean value of two independent determinations;
[b]mean value of one single run replicate (n=2) determination, for samples 7-12. Samples 1-5 were used for reproducibility assays, and thus the value presented is the mean value of all results obtained (n=5; see Table II); [c]relative error;
[d]sample No. 6 is a commercial control serum with a "recommended value" of 126 µg/dL; its concentration for GFAAS was taken from Table IV.

TABLE IV
Evaluation of Accuracy

1. Standard additions method/calibration curves slope ratio

Serum = 1.057 (5.7% proportional systematic error)
Urine = 1.023 (2.3% proportional systematic error)

2. Control samples	Recommended value	Obtained value[a] (mean+sd; n=5)	RE (%)[b]
Seronorm™ urine	28 µg/L	30.3+1.0 µg/L	+8.2
Seronorm™ serum	126 µg/dL	130.3+3.48 µg/dL	+3.4

3. Determination of copper in serum by GFAAS vs. Flame AAS[c)]

Linear regression GFAAS vs. Flame AAS: Y = 1.042 X - 2.527 (R^2 = 0.9806)
Student *t* test: *t* calculated = -2.161; *t* critical = 2.201

[a]Mean value of 5 independent replicate (n=2) determinations; [b]relative error; [c]see Table III.

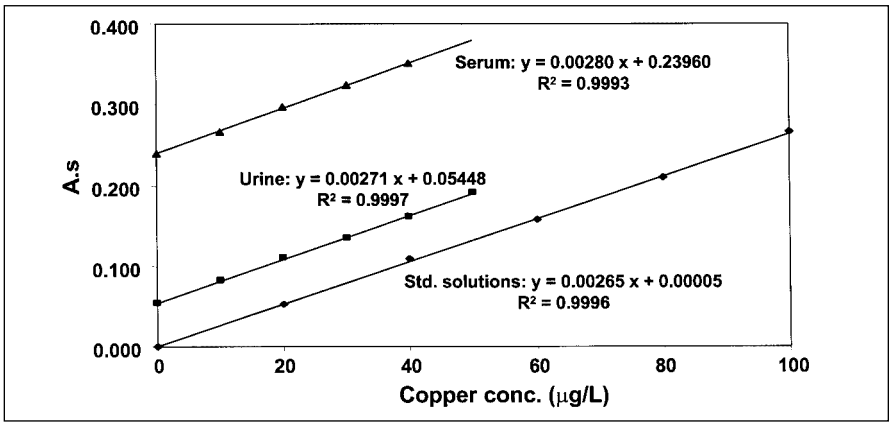

Fig. 4. Evaluation of the proportional systematic error. Relationship between the analytical signal and the copper concentration for the matrices serum, urine and 0.2% HNO_3. Concentration values correspond to the standard solution concentration before the 1+1 dilution with the diluting/matrix modifier solution.

With regard to the commercial urine control samples, it was found that the manufacturer's recommendations should be followed where transferring the solution (after reconstitution of the lyophilized samples) into plastic tubes is suggested in order to prevent contamination from the vial and the rubber stopper. Although this contamination is referred as being particularly important only for zinc and aluminum, it was found that also for copper the concentration tends to increase if the sample is kept in its original vial. For a control sample, which immediately after reconstitution provided a concentration of 30.7 µg/L ("recommended value" of 28 µg/L), the concentration of copper tended to increase continuously, reaching a final value of 41.3 µg/L after three days. Extrapolating to real samples, it seems that especially with respect to the urine samples, in which the usual copper concentrations are of about a few tens of µg/L, contact of the samples with that type of material should be avoided.

CONCLUSION

The proposed method has the main advantage of allowing the precise and accurate determination of copper in both serum and urine samples using the same instrumental and analytical conditions (same injection volume, same graphite furnace program, same calibration curve as reference, etc.). A single GFAAS analytical procedure allows this frequent demand in clinical chemistry laboratories to be fulfilled. The GFAAS method described is very important for the analysis of the critical Wilson's disease, because copper concentrations may reach such low values in a patient that they are not detectable by Flame AAS, and for pediatric patients, because the sample volume is often very limited. All validation parameters demonstrated good analytical performance of the proposed method which, in addition to being simple and quick, renders the proposed methodology suitable for routine analysis.

Received August 4, 2000.
Revision received June 8, 2001.

REFERENCES

1. J. Woo and D.C. Cannon, in J.B. Henry (Ed.) "Todd, Sanford, Davidsohn - Clinical Diagnosis and Management by Laboratory Methods," 17th edn., W.B. Saunders, Philadelphia, pp. 161-162 (1984).
2. D.B. Milne, in C.A. Burtis and E.R. Ashwood (Eds.) "Tietz Textbook of Clinical Chemistry", 2nd edn., W.B. Saunders, Philadelphia, pp. 1335-1339 (1994).
3. S.G. Chaney, in T.M. Devlin (Ed.) "Textbook of Biochemistry, with Clinical Correlations", 4th edn., Wiley-Liss, New York, pp. 1131-1132 (1997).
4. J.G. Toffaletti and P.J. Jones, in M.L. Bishop, J.L. Duben-Engelkirk and E.P. Fody (Eds.) "Clinical Chemistry - Principles, Procedures, Correlations", 2th edn., J.B. Lippincott, Philadelphia, pp. 288-290 (1992).
5. N.W. Alcock, in L.A. Kaplan and A.J. Pesce (Eds.) "Clinical Chemistry - Theory, Analysis, and Correlation", 3th edn., Mosby, St. Louis, pp. 749-750 (1996).
6. C. Terrés-Martos, M. Navarro-Alarcón, F. Martín-Lagos et al., Sci. Total Environ. 198, 97 (1997).
7. H. Hohmann and A. Klose, Labor. Med. 19, 155 (1996).
8. A. Pizent and S. Telisman, At. Spectrosc. 17, 88 (1996).
9. T. Uchida and B.L. Vallee, Anal. Sci. 2, 243 (1986).
10. S.K. Liska, J. Kerkay and K.H. Pearson, Clin. Chim. Acta. 150, 11 (1985).
11. S. Salmela and E. Vuori, At. Spectrosc. 5, 146 (1984).
12. S.A. Lewis, T.C. O'Haver, and J.M. Harnly, Anal. Chem. 56, 1066 (1984).
13. V. Hudnik, M. Marolt-Gomiscek, and S. Gomiscek, Anal. Chim. Acta 157, 143 (1984).
14. D.L. Osheim, J. Assoc. Off. Anal. Chem. 66, 1140 (1983).
15. N. Weinstock and M. Uhlemann, Clin. Chem. 27, 1438 (1981).
16. G. Rázniewska and M. Trzcinka-Ochocka, Med. Pr. 46, 347 (1995).
17. U.K. Kunwar, D. Littlejohn, and D.J. Halls, Talanta 37, 555 (1990).
18. G. Carelli, M.C. Altavista, and F. Aldrighetti, At. Spectrosc. 3, 200 (1982).
19. D.J. Halls, G.S. Fell, and P.M. Dunbar, Clin. Chim. Acta 114, 21 (1981).
20. Australian Standard AS 4205.2, 16 (1984).
21. H. Berndt, J. Baasner, and J. Messerschmidt, Anal. Chim. Acta 180, 389 (1986).
22. J. Flanjak and A. Hodda, Anal. Chim. Acta 172, 313 (1985).
23. S. Xu, M. Sperling, and B. Welz, Fresenius J. Anal. Chem. 344, 535 (1992).
24. S.K. Liska, J. Kerkay, and K. H. Pearson, Clin. Chim. Acta 151, 231 (1985).
25. A.A. Brown and A. Taylor, Analyst 109, 1455 (1984).
26. S. Lapointe and A. LeBlanc, At. Spectrosc. 17, 163 (1986).
27. J. Zhao, S. Jiang, S. Chen et al., Fresenius J. Anal. Chem. 337, 877 (1990).
28. M.B. Knowles, J. Anal. At. Spectrom. 4, 257 (1989).
29. S.A. Lewis, T.C. O'Haver, and J.M. Harnly, Anal. Chem. 56, 1651 (1984).
30. N. Velghe, A. Campe, and A. Claeys, At. Spectrosc. 3, 48 (1982).
31. O. Wawschinek and H. Höeffler, At. Absorpt. Newsl. 18, 97 (1979).
32. S.T. Wang and H.P. Demshar, Clin. Chem. 39, 1907 (1993).
33. G. Schlemer, Appl. At. Spectrosc. 1, 3E (1988).
34. G. Schlemmer, At. Spectrosc. 1, 15 (1996).
35. K.S. Subramanian, At. Spectrosc. 9, 169 (1988).
36. P. Dube, At. Spectrosc. 9, 55 (1988).
37. D.D. Koch and T. Peters Jr., in C.A. Burtis and E.R. Ashwood (Eds.) "Tietz Textbook of Clinical Chemistry", 2nd edn., W.B. Saunders, Philadelphia, p. 510 (1994).

For subscription information or back issues, write or fax:

Atomic Spectroscopy
P.O. Box 3674
Barrington, IL 60011 USA
Fax: (+1) 847-304-6865

To submit articles for publication, write or fax:

Editor, Atomic Spectroscopy
PerkinElmer Instruments
710 Bridgeport Avenue
Shelton, CT 06484-4794 USA